Report No. FRA-ORD&D 75-24

UILU-ENG 74-2032

TUNNEL DESIGN CONSIDERATIONS

ANALYSIS OF MEDIUM-SUPPORT INTERACTION

Jamshid Ghaboussi

Randall E. Ranken

Department of Civil Engineering
University of Illinois
Urbana, Illinois

NOVEMBER 1974

FINAL REPORT

Document is available to the public through the
National Technical Information Service
Springfield, Virginia 22151

Prepared for

Department of Transportation
FEDERAL RAILROAD ADMINISTRATION
Washington, D.C. 20590

NOTICE

Technical Report Documentation Page

1. Report No.	2. Government Accession No.	3. Recipient's Catalog No.
FRA-ORD&D 75-24		

4. Title and Subtitle	5. Report Date
Tunnel Design Considerations: Analysis of Medium-Support Interaction	November 1974
	6. Performing Organization Code
7. Author(s) J. Ghaboussi, R. E. Ranken	8. Performing Organization Report No. UILU-ENG 74-2032
9. Performing Organization Name and Address Department of Civil Engineering University of Illinois at Urbana-Champaign Urbana, Illinois 61801	10. Work Unit No. (TRAIS)
	11. Contract or Grant No. DOT FR 30022
12. Sponsoring Agency Name and Address Federal Railroad Administration Department of Transportation Washington, D.C. 20590	13. Type of Report and Period Covered Aug. 73-Aug. 74 Final Report
	14. Sponsoring Agency Code

15. Supplementary Notes

16. Abstract

Practical aspects of the application of analytical techniques to geotechnical problems are reviewed with emphasis on medium-support interaction problems in underground structures. It is recognized that the analysis should be carried out in several stages, reflecting the initial state of stress in the medium, the construction process and the period of operation. A finite element program called GEOSYS that is capable of performing this type of analysis is described. The capabilities and the limitations of this and other current analytical techniques in regard to the multi-stage analysis are discussed.

The results from a series of two-dimensional, plane-strain, finite element analyses of medium-liner interaction for a circular tunnel are presented. Three types of medium properties are considered, namely, linearly elastic, elasto-plastic and time-dependent. Also considered in these analyses is a simple sequence of excavation and liner placement. A comparative study of the effect of the material properties on the liner forces is made.

17. Key Words	18. Distribution Statement
Tunnel Liners, Liner-Medium, Interaction, Finite Element, Tunnel Analysis	Document is available to the public through the National Technical Information Service, Springfield, VA 22151

19. Security Classif. (of this report)	20. Security Classif. (of this page)	21. No. of Pages	22. Price
Unclassified	Unclassified	84	

Form DOT F 1700.7 (8-72) Reproduction of completed page authorized

* U. S. GOVERNMENT PRINTING OFFICE : 1973 735-104/323

PREFACE

The studies described in this report were performed by the Department of Civil Engineering of the University of Illinois at Urbana-Champaign, Urbana, Illinois during the period August 1973 to August 1974. The investigation was sponsored by the Federal Railroad Administration, Department of Transportation, through contract No. DOT FR 30022 under the technical direction of Mr. William N. Lucke.

The investigation described represents the initial analytic studies performed with the computer program described in the report. These studies will be continued and will focus on more specific problems in tunneling. The computer program was written by the firm of Agbabian Associates under the sponsorship of ARPA with ARPA Order No. 1579 and monitored by the Bureau of Mines. The program was modified for use on the IBM 360/75 computer at the University of Illinois. In this report the program has been called GEOSYS.

TABLE OF CONTENTS

LIST OF TABLES

LIST OF FIGURES

CHAPTER 1

INTRODUCTION

The capability to perform analyses of large nonlinear and time dependent systems has increased steadily in recent years through the development of modern analytical techniques using the finite element method. The potential for application of such analytical techniques to the solution of a wide range of geotechnical problems has long been recognized and is evident in the large body of literature on the subject, a survey of which is given in Ref. 4. However, a great deal needs to be done to explore the full potential of such analytical techniques and to obtain results which can be used in design of geotechnical structures. The function of the finite element method is to replace the continuous system with a discrete system with a finite number of degrees of freedom, therefore making it possible to obtain a numerical solution. The accuracy and usefulness of such numerical solutions depend on how well the mathematical model represents the real problem. In geotechnical problems the appropriate definition of the constitutive properties of geological media is an important part of the analysis and plays a controlling role in the success of such analyses. The material behavior of geological media is enormously complex. Attempts at mathematical modeling of geological media have resulted in material models which involve drastic idealizations of the behavior of real soils and rocks. Among these mathematical models are numerous linearly elastic, variable moduli, elastic-perfectly plastic, elasto-plastic strain hardening and time-dependent models. All these models are the result of attempts at improving the definition

of material behavior of geological media. This is a continuing process and in the future will result in better representations of the material behavior of geological media. Until more improved material models become available, the currently available models can be used to obtain numerical results for various problems. However, it is important to recognize the limitations of the material models and to exercise caution in interpretation and use of the numerical results.

In designing tunnel supports it is necessary to evaluate the forces expected to develop in the support system as a result of the medium-support interaction. The magnitude and distribution of forces in the support system can be evaluated by analysis of the medium-support interaction which also can provide information about the stresses and deformations in the medium and the displacement of the ground surface.

All these quantities are strongly dependent on the initial stresses existing in the ground, the method of excavation and temporary support, and the type and manner of placement of the liner or permanent support system. Therefore, the accuracy of the results of analysis depends on the availability of sufficient geological data such as the initial in situ stress condition and location and types of rock joints as well as the ability to model the process of excavation and construction. The whole process of the construction of a tunnel is a three-dimensional problem. Although theoretically the analysis of such three-dimensional problems is possible, due to the lack of sufficient data and prohibitive costs, three-dimensional analysis at the present is not advisable. Two-dimensional models of medium-support systems can be analyzed with nonlinear and/or time-dependent behavior of the medium

and considering the sequence of excavation and construction. These types of analyses can be considered an improvement over similar analyses with the assumption of linear elastic behavior of the medium. However, it is important to note that due to neglecting the three-dimensional effects, the two-dimensional models can realistically represent only certain idealized situations. In using the results of the two-dimensional analyses, judgment must be exercised as to the extent of the influence of the three-dimensional effects on the results.

In Chapter Two of this report practical aspects of the application of analytical techniques to geotechnical problems are reviewed with emphasis on the analysis of medium-support interaction problems in tunnels. It is recognized that the analysis of underground structures should be carried out at several stages, reflecting the initial state of stresses, the construction process and the operation period. The capabilities and the limitations of the current analytical techniques in application to this multi-stage analysis are discussed. In Chapter Three the results of the analysis of medium-liner interaction for a circular tunnel are presented. Three types of medium properties are considered, namely, linearly elastic, elasto-plastic and time-dependent. Also considered in these analyses is a simple sequence of excavation and liner placement. A comparative study of the effect of the material properties on the liner forces is made. Chapter Four contains a summary of the findings and certain tentative conclusions based on the case studies in Chapter Three.

CHAPTER 2

ANALYTICAL MODELING OF GROUND-STRUCTURE SYSTEMS

2.1 GENERAL

Underground structures in general possess certain unique characteristics which require specific discussion of the modeling and analysis of such structures.

Underground structures are constructed within stressed media which cover regions which, relative to the size of the structures, are usually thought of as being of infinite extent. The analytical model of the underground structure will necessarily cover a finite region of the medium with a choice of a limited number of types of boundary conditions to be imposed at the outer boundaries of the finite region. The magnitude and variation of the existing stresses in the ground before construction are often difficult if not impossible to determine accurately. The appropriate choice of an adequate region, boundary condition and initial state of stress for the purposes of analysis is not obvious. An appropriate choice of these features often requires some analytical experience with similar types of analysis and a general awareness of the sensitivity of the results to the variation of such features.

Unlike other types of structures, the loading on underground structures is not known a priori but is a result of medium structure interaction. In consideration of medium-structure interaction the sequence of excavation and construction are of great importance and must be reflected in the analysis. The quantities of interest--such as the

forces acting on the structure or certain displacements--are functions of initial stresses and the sequence of excavation and construction.

The analysis of the mathematical model of the underground structure should be carried out in three phases, each representing a distinct stage under significantly different conditions. The three stages are as follows:

1. Initial Phase--The aim of this phase of analysis is to determine the initial state of the stress existing in the ground prior to the construction of the underground structure. This is accomplished by the analysis of the pre-excavation configuration subject to the self-loading of the medium and other possible types of loading such as the weight of any existing adjacent structures.
2. Construction Phase--In this phase of the analysis the actual sequence of excavation and construction is simulated. This phase starts from the initial state and covers the period leading to the completed underground structure.
3. Operation Phase--The completed structure may be subjected to various possible loading conditions during its useful life arising from the operation of the structure or from external influences.

2.2 SOLUTION

The application of the finite element method to modeling of the underground structure results in a discrete system with a finite number of

degrees of freedom. In the analysis of underground structures the system is expected often to be nonlinear. In addition to nonlinear material behavior other discrete nonlinearities are expected to develop such as the change of geometry and boundary conditions. The change of geometry due to simulation of excavation and construction can also be treated as a discrete nonlinearity.

A general solution method is discussed here which is capable of incorporating the above nonlinearities in any arbitrary combination. The system is solved by the repetitive application of the following incremental equation of equilibrium with equilibrium correction.

$$K\Delta u = P - \sum \int_v B^T \sigma \, dv \qquad (2.1)$$

In which

K = stiffness matrix for the whole structure

Δu = increment of the displacement vector

P = load vector

B^T = transpose of the element strain/displacement transformation matrix

σ = element stress vector.

In the second term on the right hand side of Eq. 2.1 the integral is carried out over the volume, v, of each element and the summation is over all the elements in the model and symbolizes the direct assembly of the elements.

The following special solution scheme can be developed from Eq. 2.1 by controlling the rate of the application of loading.

1. Pure Incremental--When the loading on the system is increased

by specified increments, the application of Eq. 2.1 becomes equivalent to a pure incremented technique.

2. Iterative--Iteration can be carried out by using Eq. 2.1 repetitively with a constant loading equal to the final value of the loading.
3. Combined Incremental and Iterative--The loading can be applied incrementally but after each increment some iterations can be done by keeping the load constant at that level for several steps.

The pure incremental method produces some unbalanced forces at the end of each step resulting in step errors. However, the accumulation of the step errors is prevented by the equilibrium correction which takes place in the following step. The magnitude of the step errors depends on the severity of the nonlinearity and the size of the increment. Iteration at a constant loading reduces the step errors and the unbalanced forces. Convergence is achieved when a specified norm of Δu or when the right hand side of Eq. 2.1 falls below a specified level.

Another important factor in controlling the accuracy and efficiency of the solution methods is the frequency of the reformation of the structural stiffness matrix (stiffness update). The structural stiffness for nonlinear problems is in general a function of the state variables, however the reformulation and decomposition of the stiffness matrix is computationally very costly and in practice the stiffness matrix is only updated at an interval of several steps. The updating of the stiffness matrix in general reduces the step error in the pure incremental technique and increases the rate of convergence during iteration.

The optimum solution scheme in terms of accuracy and efficiency is usually a combination of incrementation and iteration with a certain stiffness update interval. However, this combination is dependent upon the specifics of a given problem and general rules do not exist for determination of an optimum solution scheme. The loading should be applied in increments small enough that large changes in the stress condition do not occur and few iterations will be required. However, in some cases this cannot be controlled. An example of such a case is the excavation which must be done in one step but may result in large changes in the stress condition. After the excavation step, iterations are required in order to reduce the unbalanced forces.

A cycle of solution using Eq. 2.1 involves the following operations.

1. Determine the strain increments for all the elements from the displacement increments of the previous step using the strain/displacement matrix B.

$$\Delta\varepsilon = B\,\Delta u$$

2. Using the strains and stresses from the previous step and current strain increments, compute the tangent material property matrix C_t and the stress increments

$$\Delta\sigma = C_t \Delta\varepsilon$$

The relation between the stress increments and the strain increments is nonlinear and the above computation may have to be carried out by incrementation or iteration.

3. If a stiffness update is required, compute the element stiffnesses and assemble into a global stiffness matrix using the current tangent material property matrix.

$$K = \sum \int B^T C_t \, B dv$$

4. Compute the internal resisting force vector from current stresses.

$$F = \sum \int B^T \sigma \, dv$$

5. Solve for the displacement increments.

$$K\Delta u = P - F$$

6. Repeat computation steps 1 through 5 for the next cycle.

In the computations in steps 3 and 4 only those elements are considered which are active at the current step.

2.3 INITIAL STATE

The first step in the analysis of underground structures is to simulate the existing stress condition in the ground prior to the excavation and construction. This is a difficult task and often some compromise has to be made since the stresses in the ground are a result of the past geological history. The ground has been subjected to a stress path during its geological history and often such stress paths cannot be determined. Even if the past stress path is known, it is doubtful whether the ground stress conditions can be duplicated with the present analytical capabilities.

Analytically the initial state of stresses is determined from the pre-excavation configuration subject to the weight of the medium and other types of loading such as the effect of adjacent structures. For a linear medium the initial state can be determined in one step. In case the medium is assumed to be nonlinear, depending on the nonlinear properties and the level of loading, below a certain depth yielding can be expected to occur. As a result of such yielding the relative magnitude of horizontal stress will increase with depth and will be greater than the linear case with the same properties. This condition will amount to an increase of the value K_o (the ratio of horizontal and vertical stresses) with depth. Of course, it must be recognized that the above discussion applies only to the case of simple soil profiles, namely a uniform isotropic or horizontally layered soil condition. Initial stress states for complex geological conditions are considerably more difficult to determine. The initial ground stress state will be more complicated in the cases of a non-horizontal ground surface, orthotropic medium properties, non-uniformly layered soil profiles and the existence of stress-limiting features such as rock joints or the proximity of faults. The analysis of the initial stress state for such complex geological conditions may require the use of a combination of force and displacement boundary conditions.

The analysis of the initial state in a nonlinear medium should be carried to the final equilibrium state which may require some iterations or incremental application of the self loading or a combination of both. In a creeping medium the initial state of stress in the ground can be considered to have resulted from the creeping of the medium for a long

period of time under the self loading or other external effects. Therefore it can be assumed that the creeping has effectively terminated. In the analytical simulations of the initial state, creeping of the medium will take place under the application of the self-loading, however the analysis must be carried to a reasonable period of time corresponding to the termination of the creep. In some cases at the time of the construction creeping of the medium due to prior construction may still be taking place. The effect of such prior disturbance should be considered in addition to the effect of the self-loading.

2.4 SIMULATION OF EXCAVATION AND CONSTRUCTION

The magnitude and the distribution of the long term forces acting on any underground structure as well as internal forces in such structures are significantly affected by the sequence of excavation and construction leading to the completion of the underground structures. This is more so in cases where yielding and subsequent redistribution of stresses is expected to occur in the medium. The analysis of the completed structure without considering the construction sequence will not yield satisfactory results mainly because the forces acting on the structure cannot be determined accurately and also because the stress paths will be different from the stress paths in the real structures.

The technique for the simulation of construction using the finite element method was initially developed by Clough and Woodward (2) in an analysis of the construction of earth dams. The technique has been

used for the analysis of numerous geotechnical problems involving the simulation of excavation as well as construction. The simulation technique has been used in the analysis of the incremental construction of earth dams (10), large open excavations (8), braced excavations (3) and excavation of large underground openings for mining installations (1).

The purpose of the analysis of the excavation process is to determine the change of state (displacements, strains, and stresses) as a result of the removal of a stressed portion of the system. Before the excavation (pre-excavation stage) certain stresses act on the surface which is to form the boundary of the excavated region. These stresses vanish upon the completion of the excavation (post-excavation stage) if no internal support or pressure is immediately applied. Using the finite element method, some researchers (3) have simulated the process of excavation by computing the forces acting on the excavation surface at the pre-excavation stage and subsequently applying the opposite of those forces to the model of the post-excavation stage which is formed by the removal of the excavated portion. However, such techniques can be used only in linear analyses and involve combersome and lengthly multi-stage computer analysis of the different stages of the excavation and construction.

A more general approach to the simulation of excavation and construction is to treat the problem as a nonlinear one. The source of nonlinearity in this case is the change of the geometry of the system. Therefore a general solution scheme for nonlinear problems can be used. The incremental equation with equilibrium correction for a finite element system is given by Eq. 2.1. As discussed previously this equation is valid for nonlinear as well as viscous materials. For the portions of the system

to be excavated and/or constructed, elements are assigned initially and the analysis is carried out incrementally. The elements in the portions to be excavated are active originally and at the appropriate step when the excavation is to take place these elements are deactivated, i.e., they are not assembled in the remainder of the analysis. The support is simulated using a reverse process; the elements are inactive initially and they are activated at the step when the support is to be installed. The activated elements may already be stressed to simulate prestressing, such as is the case with tensioned rock bolts.

In linear systems one step of the solution of Eq. 2.1 at each step of excavation and construction is sufficient to satisfy equilibrium. However, in the presence of a nonlinear medium in the system several equilibrium iterations may be required after each step of excavation and construction. The number of equilibrium iterations depends on the extent of the region of excavation or construction. Obviously a larger region of construction activity will cause a larger stress change, requiring a greater number of iterations in order to satisfy equilibrium. In a creeping medium the time history of the state variable is evaluated by a time marching scheme. The excavation and construction will take place at steps corresponding to real time. After each step of construction activity the rate of change of stress will be a maximum and therefore a smaller time step must be used in these regions of the time history.

2.5 MATERIAL PROPERTY MODELS

2.5.1 GENERAL

Soils and rocks exhibit a complex nonlinear and often time-dependent material behavior. Mathematical modeling of the material behavior of soils and rock is difficult and necessarily involves certain simplifying assumptions. The simpler material models are associated with more idealizations and assumptions. In the hierarchy of the material models simplifying assumptions are removed in constructing higher levels of material models which are capable of simulating more features of the material behavior. The improvement of the material models for soils and rocks is the subject of current active research and the search for better material models continues. However, the more complex the material model is, the more difficult and costly it is to use such a material model in the analysis.

In finite element analyses of nonlinear systems, the tangent material property matrix is used which relates the increment of strains and the increment of the stresses.

$$\Delta\sigma = C_t \, \Delta\varepsilon \qquad (2.2)$$

The total stresses are the accumulation of the stress increments. The structure of the tangent material property matrix depends on the mathematical model of the material behavior. In the remainder of this section various aspects of several material models are discussed.

2.5.2 LINEAR ELASTIC

The simplest material model is linearly elastic material behavior. Due to the ease of formulation, this material model has been widely used in the analysis of geotechnical problems including underground structures. Material behavior of geological media can reasonably be assumed to be linearly elastic at low stress levels or when the changes in the stress levels are small. However, this range of applicability depends on the type of the geological medium. For a small change in the stress level the material can be assumed to behave elastically with moduli dependent on the stress level. The analysis of geotechnical problems using a linearly elastic model will provide preliminary results for design. However, the sufficiency of such results can be established only by comparison with field observations or the results of analysis using improved material models.

If the material is assumed to be isotropic, only two material constants are sufficient to establish the material property matrix which will have the following form.

$$\begin{Bmatrix} \sigma_{xx} \\ \sigma_{yy} \\ \sigma_{zz} \\ \sigma_{xy} \\ \sigma_{yz} \\ \sigma_{xz} \end{Bmatrix} = \begin{bmatrix} B & \lambda & \lambda & & & \\ \lambda & B & \lambda & & & \\ \lambda & \lambda & B & & & \\ & & & G & & \\ & & & & G & \\ & & & & & G \end{bmatrix} \begin{Bmatrix} \varepsilon_{xx} \\ \varepsilon_{yy} \\ \varepsilon_{zz} \\ \varepsilon_{xy} \\ \varepsilon_{yz} \\ \varepsilon_{xz} \end{Bmatrix} \quad (2.3)$$

where $B = K + \frac{4}{3} G$ and $\lambda = K - \frac{2}{3} G$ and K and G are the bulk and shear moduli respectively.

2.5.3 VARIABLE MODULI

In variable moduli models the nonlinear behavior is represented by the equivalent elastic moduli which are functions of the history of stresses and strains. One such model is proposed in Ref. 11 in which the bulk and shear moduli are assumed to be variable.

$$\Delta\sigma_{ij} = (K - \frac{2}{3} G)\, \delta_{ij}\, \Delta\varepsilon_{kk} + 2G\, \Delta\varepsilon_{ij} \qquad (2.4)$$

The bulk modulus has different values for loading and unloading, and is determined by the previous maximum of the mean stress. The loading bulk modulus is a function of the volumetric strain. The shear modulus also takes two different values for the loading and unloading. The shear modulus is a function of the second invariant of the deviatoric stress and the volumetric strain or stress.

The implementation and use of the variable moduli models in the finite element method is relative easy and in certain cases satisfactory results can be obtained. However, for certain stress paths the uniqueness cannot be proved. The material constants for the variable moduli models are determined by data fitting of experimental results.

Other simpler bi-modular models have also been used effectively in the analysis of underground structures. One such model is referred to as the "no-tension" model (17). In this model the principal tensile stresses in the system are removed iteratively and subsequently the material is treated

as an orthotropic medium. The no-tension material model can be used to effectively simulate the overburden stresses acting on tunnel liners, which result from the weight of the medium above the liner due to disturbance of the medium in that region by the installation of the tunnel.

2.5.4 ELASTO-PLASTIC

The basic feature of an elasto-plastic model is a yield function which defines a surface in the stress-space. Points within this surface are assumed to correspond to elastic behavior, whereas yielding takes place when the stress point lies on this surface, satisfying the yield condition. The yield condition is defined by the following equation.

$$f(\sigma_{ij}, K) = 0 \tag{2.5}$$

in which K is the hardening parameter. A flow rule also has to be assumed to define the rate of the plastic strain. The most commonly used flow rule is the associated flow rule in which the plastic potential is assumed to be the same as the yield function. This specifies the increment of the plastic strain to be normal to the yield surface as given by the following relation.

$$d\,\varepsilon^{p}_{ij} = d\,\lambda\,\frac{\partial f}{\partial \sigma_{ij}} \tag{2.6}$$

Following a standard derivation (for example see Ref. 18) the relation between the increment of stresses and the increment of strains can be established through an elasto-plastic tangent material property matrix.

$$\Delta\sigma = C_{ep}\,\Delta\varepsilon \tag{2.7}$$

in which

$$C_{ep} = C - \frac{C\, d\, d^t\, C}{\Lambda + d^t\, C d} \tag{2.8}$$

C = elastic material property matrix

$$d = \frac{\partial f}{\partial \sigma_{ij}}$$

Several elasto-plastic models have been proposed in the past to represent the behavior of geological media. Some of the better known models are discussed in the following.

Drucker-Prager Model--This model, which is a generalization of the Mohr-Coulomb yield criterion, is defined by the following yield function (6).

$$f = \sqrt{J_2'} + \alpha J_1 - k \tag{2.9}$$

in which $J_1 = \frac{1}{3}\sigma_{ij}\,\delta_{ij}$ is the first invariant of stresses and $J_2' = \frac{1}{2} s_{ij} s_{ij}$ is the second invariant of deviatoric stresses $s_{ij} = \sigma_{ij} - \delta_{ij} J_1$. The material constants α and k are related to cohesion and angle of friction. With the appropriate choice of the material constants this model is capable of simulating the material behavior of a range of types of geological media. However, the Drucker-Prager model represents the material behavior more accurately at the lower stress ranges. The proportional increase in the shear strength with increasing mean pressure does not appear to be valid at higher stress ranges. The use of the associated flow rule with this model results in a plastic strain increment vector, the horizontal component of which is in the positive direction of J_1 and as a result it corresponds to

a volume increase. Real soils exhibit contraction as well as dilation under shear stresses, depending on the void ratio and mean pressure. This behavior cannot be simulated by the Drucker-Prager model.

Modified Drucker-Prager Model--Modifications to the Drucker-Prager model have been made in order to limit the shear strength for high values of mean pressure. One such model proposed by Nelson and Baron (12) has the following yield function

$$f = \sqrt{J_2'} + \alpha J_1 \left(1 + \frac{J_1}{2c}\right) - k \qquad \text{for } J_1 \geq c$$

$$f = \sqrt{J_2'} - k - \frac{\alpha c}{2} \qquad \text{for } J_1 < c \tag{2.10}$$

For values of J_1 less than c this model corresponds to the Mises yield function. A similar model has been proposed by Di Maggio and Sandler (5) in which the yield function asymptotically approaches the Mises yield function.

For low mean pressure levels, these yield functions are close to the Drucker-Prager model. However, the rate of dilatancy in these models is a function of mean pressure and less than the rate of dilatancy in the Drucker-Prager model.

Hardening Models--The elastic-perfectly plastic models discussed above will not produce hysteresis under hydrostatic loading and unloading. Also, when the associated flow rule is used they will produce only dilatancy under shear. However, real soils display hysteresis under hydrostatic loading and unloading and they contract or dilate under shear, depending on plastic volumetric strain. In order to produce these effects the yield function must

cross the J_1 axis. The first such model was proposed by Drucker, Gibson and Henkel (7). They added a strain hardening cap to the Drucker-Prager yield function. Di Maggio and Sandler (5) formulated a strain hardening model which consists of a perfectly plastic Modified Drucker-Prager yield function and a strain hardening cap. The cap expands and contracts as a function of volumetric plastic strain. This model produces contractancy for plastic loading over the cap. Roscoe and his co-workers at Cambridge University (15) have also developed a strain hardening plasticity model which is capable of simulating similar features of soil behavior.

These models require additional material parameters which must be determined indirectly and cannot be measured directly from conventional experiments. Although these models have been used with the finite element method by some researchers, more experimental and analytical studies are needed to explore their full potentials in solving geotechnical problems.

CHAPTER 3

CASE STUDIES

3.1 GENERAL

The medium-support interaction type of analysis is an approach to tunnel liner design that represents a potential improvement in design procedure since it considers in a more rational manner not only tunnel geometry and loading, but also the material properties of the medium and the liner.

Using both closed form and discrete element methods that allowed for consideration of medium-support interaction, Paul, et al (13) investigated the distribution of forces and deformations in circular tunnel liners embedded in an elastic medium. In this chapter the results of similar studies are presented in which, in addition to linear-elastic material properties, elasto-plastic and time-dependent material behavior were also considered.

A considerable amount of work has been done in the last few years in an attempt to obtain realistic analytic models of the constitutive behavior of soils and rocks. Such behavior has been found to be very complex and, while advances have been made, no widely applicable models have been obtained. Nevertheless, improved approximations to real behavior can be obtained if the stress-strain-time model most applicable to the problem being considered is selected from the models available and used in place of, or in addition to, the linear-elastic model.

Closed form solutions to the interaction problem of a lined tunnel in other than linear-elastic materials do not exist. Numerical techniques such as the finite element method must be used if other types of material behavior are considered. The finite element method was used exclusively in this study.

This chapter describes some preliminary results of an investigation into the response of a circular tunnel liner embedded in a medium whose stress-strain-time behavior was described by:

1. A linear-elastic model (one case);
2. A nonlinear (elasto-plastic), time-independent model (two cases);
3. A time-dependent (viscoelastic) model (two cases).

For each case the material model that was used is discussed and the resulting distributions of liner external stresses and internal forces are given.

These analyses were of the two-dimensional, plane strain type. It is a radical simplification to reduce a three-dimensional problem to two dimensions. However, because the difficulties associated with a three-dimensional analysis are so great, and because the plane strain condition is valid for cross sections away from the tunnel face, the two-dimensional analysis has been widely used. Two things must be kept in mind, however. First, that this type of analysis is not applicable to cross sections near the tunnel face (within one or two diameters). Second, that the plane strain analysis, in the form generally used, cannot properly take into

consideration the deformations and stress changes that the surrounding medium experiences before the liner is installed (instantaneous and/or time-dependent phenomena occurring between the liner and the face and even ahead of the face). Thus, when using the results of a two-dimensional analysis, sound engineering judgment must be exercised to evaluate the applicability of the analysis results to the real three-dimendional problem.

Although the ultimate goal of these investigations is to provide useful information that can be used in the design of tunnel supports, the results presented here are considered tentative and are not intended for use in design at this time. They apply to too narrow a range of material parameters to be truly useful. In the near future a much wider range of material properties and, in some cases, more realistic material models will be evaluated.

3.2 FINITE ELEMENT AND MATERIAL BEHAVIOR MODELS

3.2.1 GENERAL

The tunnel support considered in this investigation, illustrated in Fig. 3.1a, was a circular, unreinforced concrete liner of 20 ft (6 m) mean diameter and 1 ft (30 cm) thickness. The dimensions were selected so that the liner would be fairly representative of those constructed for urban mass transportation systems. In all cases the liner was assumed to behave elastically. The values selected for the modulus of elasticity and Poisson's ratio of the liner were 2×10^6 psi (13.8×10^9 Pa) and 0.15 respectively.

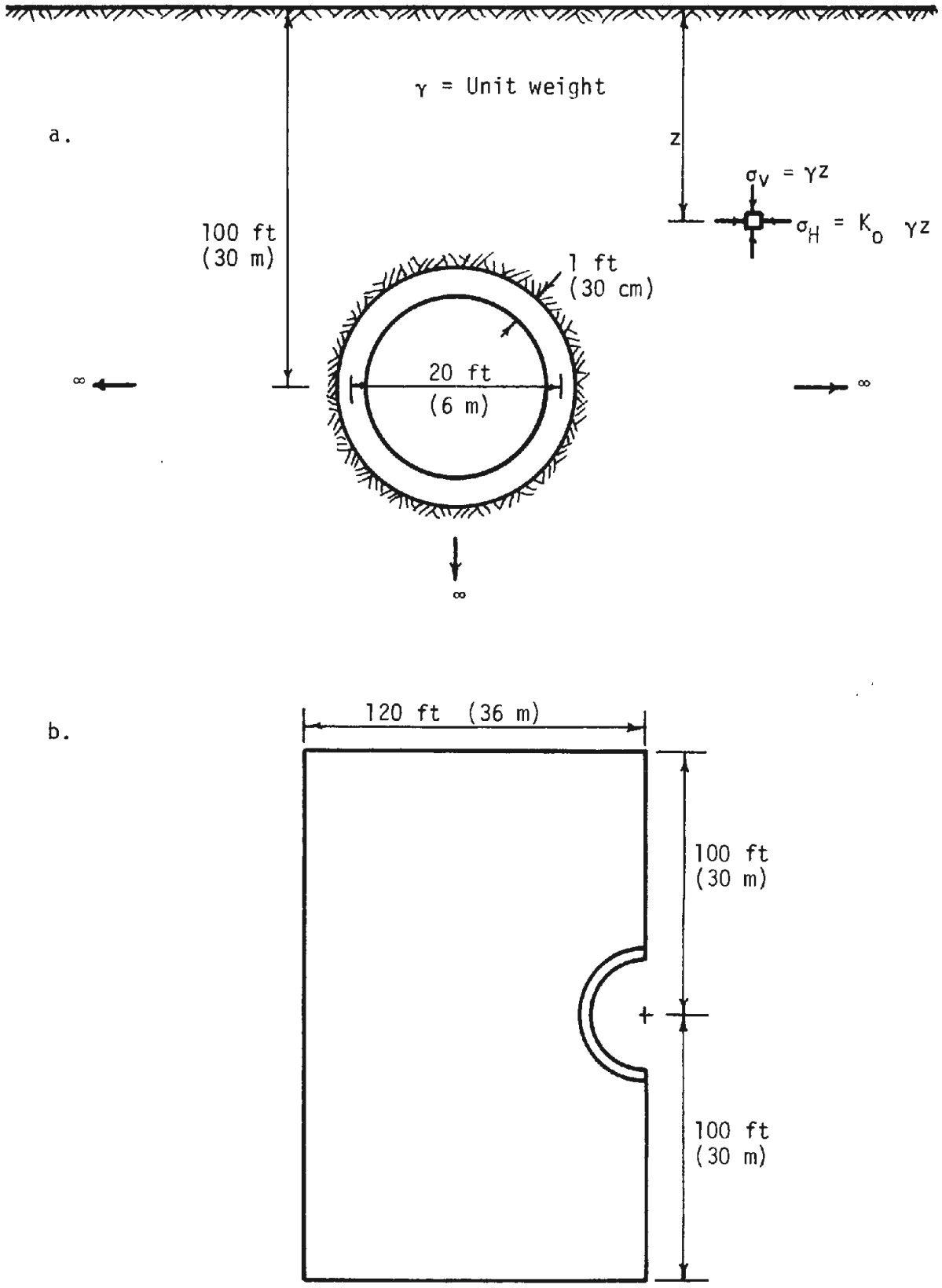

FIGURE 3.1 (a) SEMI-INFINITE MEDIUM-LINER SYSTEM TO BE MODELED AND (b) FINITE SYSTEM SELECTED FOR ANALYSIS

The liner was embedded in a semi-infinite, homogeneous, isotropic medium at a depth, from surface to tunnel axis, of 100 ft (30 m). The properties of the medium, described in following sections, were selected so as to be more representative of soil than rock. No attempt was made, however, to model any specific soil mass.

The stress at any point within the medium was considered to be a function of the weight of the overlying soil. Prior to any disturbance, the vertical stress at any point was equal to the product of the depth, z, of that point below the ground surface and the unit weight, γ, of the soil. The horizontal stress at the same point was equal to the coefficient of earth pressure at rest, K_o, times the vertical stress. Thus, the increase in stress with depth was considered.

Both the geometry of the problem and the loading were symmetrical about the vertical axes. Thus, it was possible to effectively "cut the problem in half" along this axis and reduce the amount of calculation required to analyze the problem completely.

The finite element procedure cannot be applied to an infinite or semi-infinite space. Therefore, as shown in Fig. 3.1b, a finite block of soil around the tunnel was selected for study. The dimensions of the block were chosen such that the boundaries were sufficiently far from the tunnel to insure that there would be no significant effect on the liner by events occurring beyond the boundaries and vice versa.

Figure 3.2 is a reproduction of the finite element mesh, or model, used in this investigation. Two-dimensional, plane strain, quadrilateral

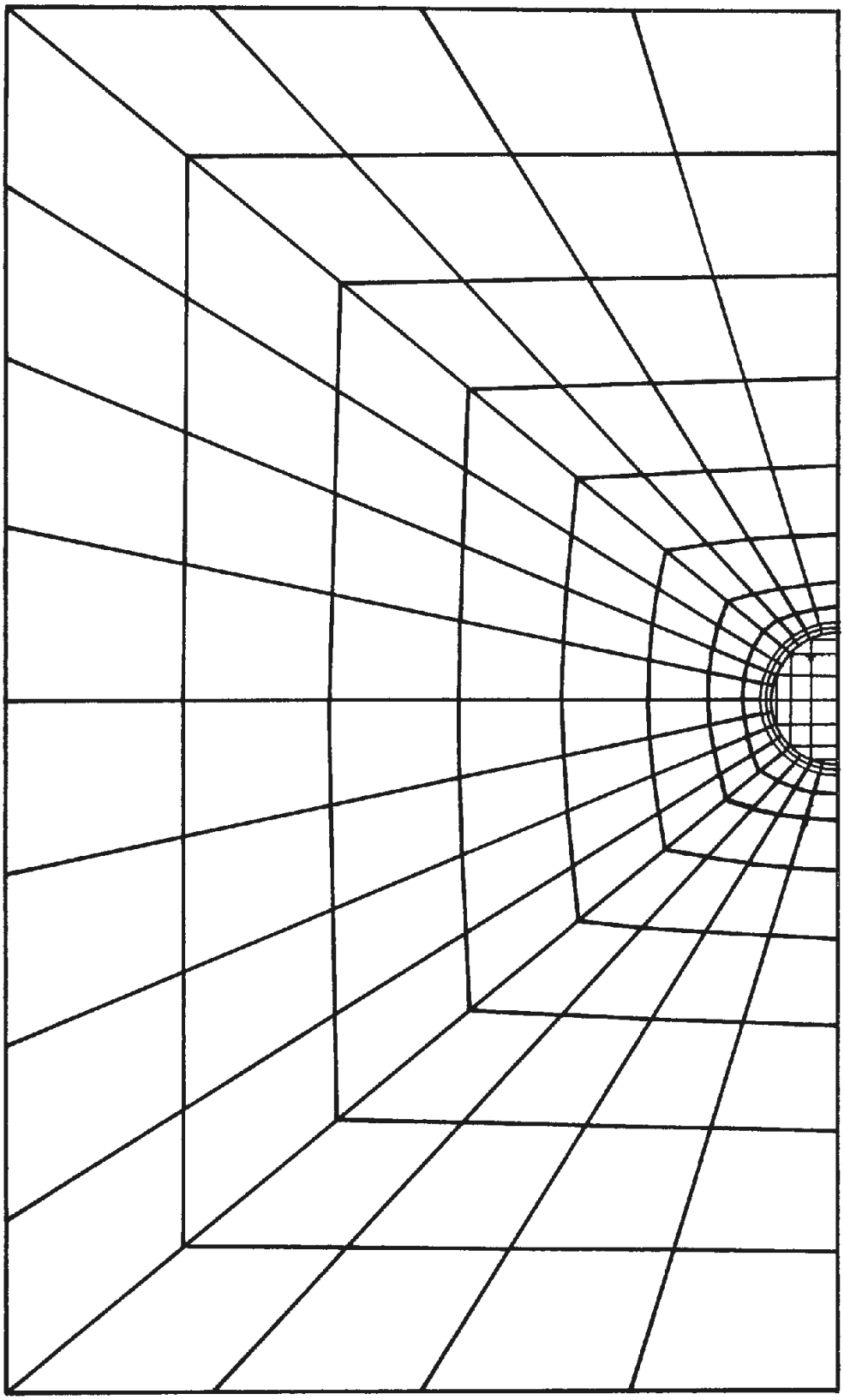

FIGURE 3.2 THE FINITE ELEMENT MESH

elements were used for both the soil and the liner. Displacements along the mesh boundaries were restricted in a manner consistent with realistic behavior. The top boundary, which represents the ground surface, was left free. The right boundary, which is a line of symmetry, was restrained from moving in the horizontal direction. The same restraint was applied to the left boundary during application of the dead load, allowing the medium to deform vertically. In addition, restraints against vertical movements were imposed on the left boundary once deformations due to the dead load had ceased. The bottom boundary was completely fixed.

Because the analyses were two-dimensional, the excavation process mentioned throughout this chapter does not refer to excavation of the tunnel face. Rather, this excavation process is a technique used to simulate the existence of a tunnel in a stressed medium.

Many past analyses of the medium-support interaction problem have considered tunnels that existed in the medium before the medium was stressed. In reality, of course, tunnels are advanced through media which are already stressed. In this study the stresses were applied to the medium first, and then the cross section of the tunnel was "excavated" and the liner was installed.

This sequence was achieved by performing each analysis in a series of calculation steps. The first step always consisted of applying stress, corresponding to the self-weight of the soil, to the entire soil mass. This constituted the initial in situ stress state of the undistrubed soil mass. One or more calculation steps then followed. These steps were used to

deactivate certain "soil" elements to form the tunnel (excavation), to activate "liner" elements to form the liner, or to allow the system to come to equilibrium. It can be seen from Fig. 3.2 that the finite element mesh was set up so that the tunnel could be excavated and the liner installed at the desired location. The following example step series and Fig. 3.3 illustrate the procedure used.

Step 1: All elements shown in Fig. 3.2 are assigned the properties of soil and the dead load is applied.

Step 2: No changes are made. This is an equilibrium iteration.

Step 3: Those elements within the boundary of the intended liner's exterior surface are deactivated (excavation).

Step 4. Those elements comprising the liner are activated (liner placement).

Step 5: No changes are made. This is an equilibrium iteration.

The number and sequence of steps required vary with the type of analysis being performed. The finite element program used in this study performs the above series of steps automatically. Thus, it is not necessary to make more than one computer run to get final results.

3.2.2 LINEAR-ELASTIC MODEL

The most widely used model of material behavior has been the linear-elastic model. By assuming a linear relationship between stress and strain (see Fig. 3.4) the number of parameters required to describe material behavior is held to a minimum. This simplifies the analytical approach to

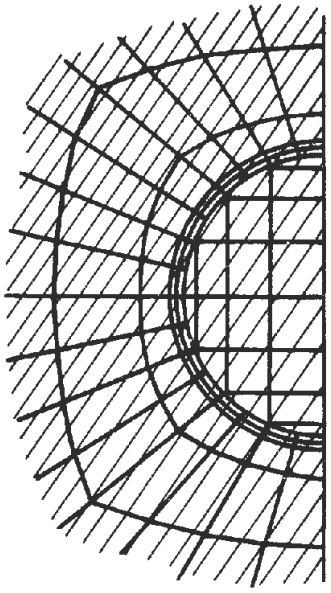

Dead load

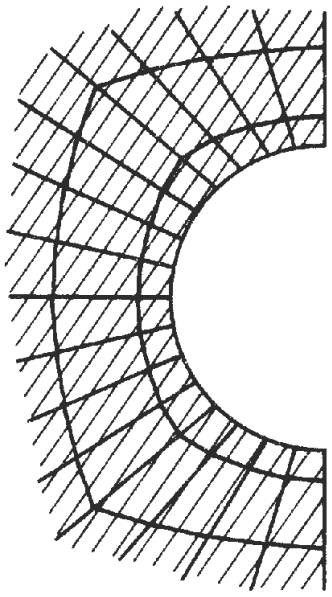

Excavation

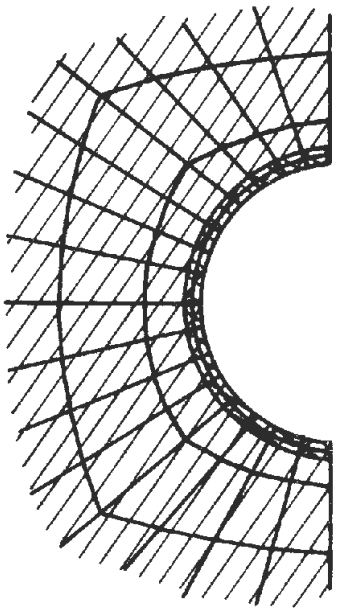

Liner placement

FIGURE 3.3 CHANGES MADE IN THE FINITE ELEMENT MESH DURING A LOAD STEP SERIES

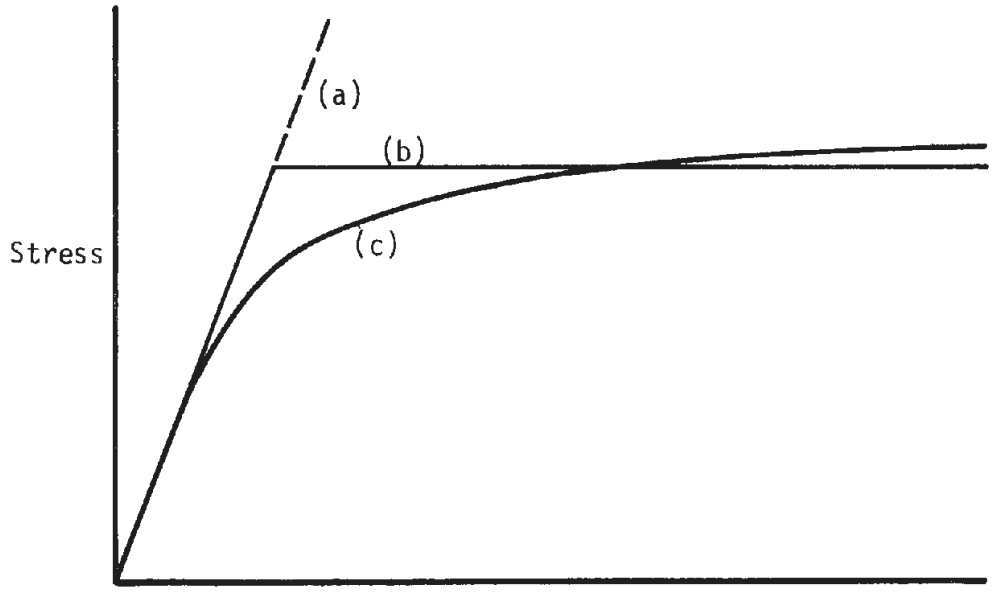

(a) Linear-elastic model

(b) Elasto-plastic model

(c) Loose sand or normally loaded clay (low sensitivity)

(d) Dense sand or highly overconsolidated clay

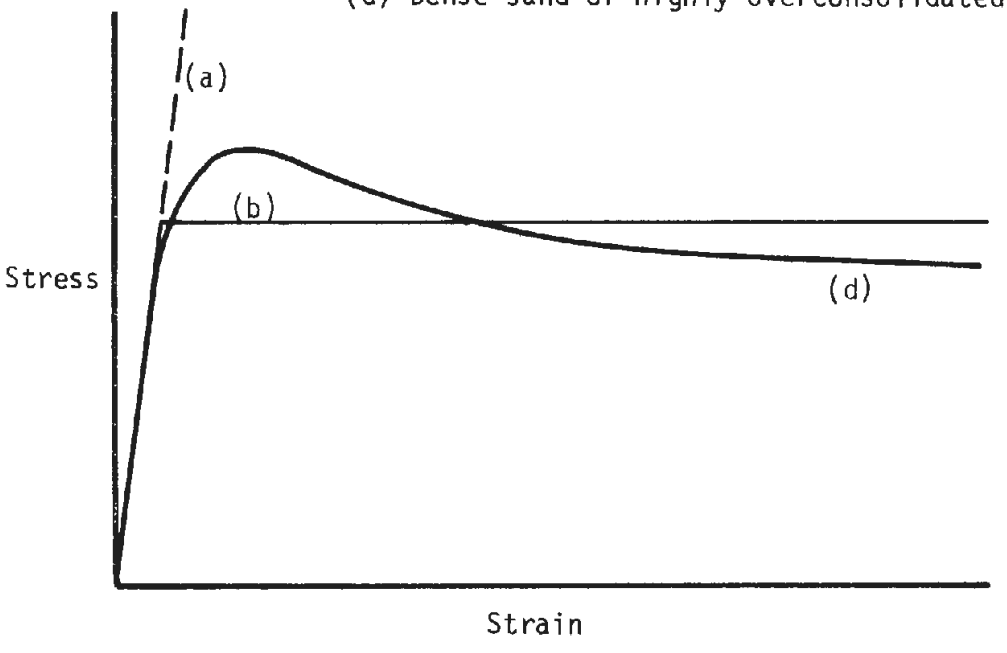

FIGURE 3.4 IDEALIZED STRESS-STRAIN CURVES AND TYPICAL CURVES FOR REAL SOILS

the problem and makes possible the formulation of closed form and finite element solutions that are efficient and easy to use.

For this case, both the liner and the medium were assumed to behave elastically and independently of time. The stress-strain behavior of both "liner" and "soil" elements was defined by specifying values for the bulk and shear moduli, these quantities being determined from the elastic modulus and Poisson's ratio. These values and the selected material unit weights are given in Table 3.1.

From these values and the dimensions of the liner Compressibility and Flexibility ratios (which have been defined in Refs. 13, 14) of 0.16 and 11.0, respectively, were obtained. These values indicate that the liner falls in the transition zone between rigid and flexible behavior as defined by Peck, et al. (14)

Since it was assumed that the material behavior in this case was independent of time, only two steps were required to complete the analysis. The first step corresponded to step 1 as described in Section 3.2.1 (dead load application). The second step corresponded to the combined steps 3 and 4 (excavation and installation of liner).

TABLE 3.1

STRESS-STRAIN PROPERTIES AND UNIT WEIGHTS USED IN THE LINEAR-ELASTIC ANALYSIS

	Elastic modulus, E psi (Pa)	Poisson's ratio ν	Bulk modulus, B psi (Pa)	Shear modulus, G psi (Pa)	Unit weight, γ lb/ft^3 (kg/m^3)
Liner	2×10^6 (13.8×10^9)	0.15	9.5×10^5 (6.6×10^9)	8.7×10^5 (6.0×10^9)	150 (2400)
Medium	1.5×10^4 (10.3×10^7)	0.333	1.5×10^4 (10.3×10^7)	5.6×10^3 (3.4×10^7)	120 (1920)

3.2.3 ELASTO-PLASTIC MODEL

One of the first steps than can be taken in an attempt to improve the applicability of solutions to the medium-structure interaction problem is to introduce nonlinear material properties to the analysis. It is known that most soils and rocks exhibit linear stress-strain behavior only when subjected to low stress levels. For most underground construction projects in soil the stresses in the medium are high enough so that the assumption of linear-elastic material behavior is not justified.

There are several models that can be used to simulate nonlinear material behavior analytically or numerically. The one used here was an elasto-plastic model. For this model the medium was assumed to behave elastically until a specified failure condition was satisfied, whereupon yielding would occur and perfectly plastic behavior would commence. The type of stress-strain curve that results is shown in Fig. 3.4. The liner was assumed to behave elastically.

The yield condition utilized by this model is a modified form of the Drucker-Prager model which is, in turn, a three-dimensional generalization of the Mohr-Coulomb failure criterion (5). Figure 3.5 illustrates the three different failure surfaces. In Fig. 3.5a the terms c and ϕ are for the plane strain case and compressive stresses are positive. In Fig. 3.5b and c compressive stresses are negative. The modified Drucker-Prager failure criterion is as follows:

$$\text{For } J_1 \geq m,\ f_1 = \ell\left(1 - \left|1 - \frac{J_1}{m}\right|^2\right) + k - \sqrt{J_2'} \geq 0 \qquad (3.1)$$

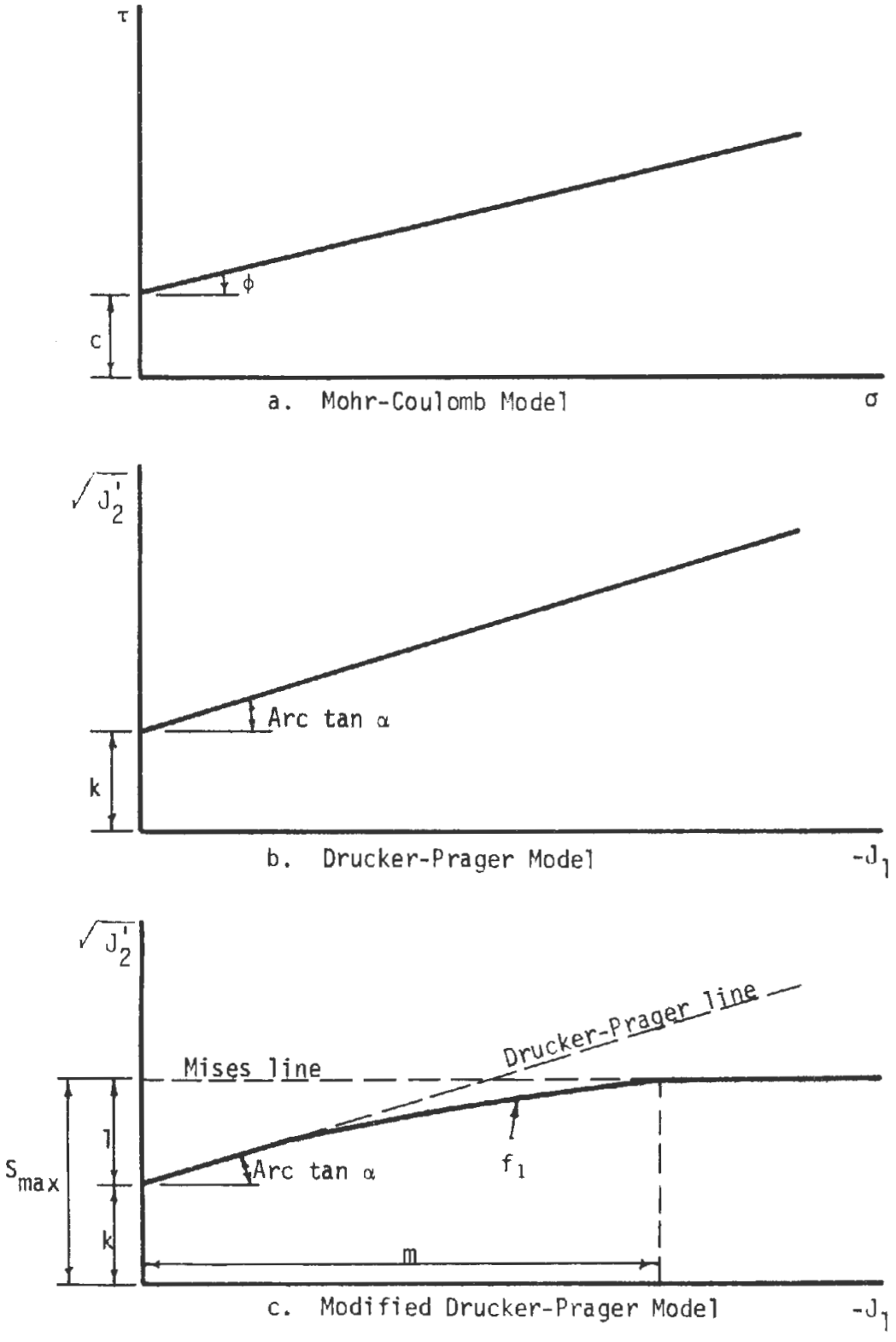

FIGURE 3.5 MOHR-COULOMB, DRUCKER-PRAGER, AND MODIFIED DRUCKER-PRAGER YIELD SURFACES

$$\text{For } J_1 \leq m, \; f_1 = \ell + k - \sqrt{J_2'} \geq 0 \tag{3.2}$$

$$J_1 = \sigma_{xx} + \sigma_{yy} + \sigma_{zz} \tag{3.3}$$

$$J_2' = -\frac{1}{6}\left[(\sigma_{xx} - \sigma_{yy})^2 + (\sigma_{yy} - \sigma_{zz})^2 + (\sigma_{zz} - \sigma_{xx})^2\right] - \sigma_{xy}^2 \tag{3.4}$$

The quantity J_1 is the first invarient of the stress tensor. The quantity J_2' is the second invarient of the deviatoric stress tensor. At values of $-J_1$ near the origin, the yield surface, f_1, (Fig. 3.5c) corresponds to that of the Drucker-Prager model wherein the failure envelope, f_1, varies with confining pressure, J_1. As $-J_1$ increases in magnitude, f_1 diverges from the Drucker-Prager line and gradually approaches the Mises yield function. For $-J_1$ values to the right of m, the shear strength is a constant, S_{max}, and is independent of confining pressure. For the majority of materials whose strength is a function of their angle of internal friction, ϕ, this latter condition is achieved only at exceedingly high confining pressures, much higher than those encountered in most underground construction projects.

The yield surface, f_1, is defined within the finite element program by specifying the three quantities, k, ℓ and m. These values may be obtained by running a series of triaxial tests on soil or rock samples and plotting the results (stresses at failure) in the $\sqrt{J_2'}$ vs. $-J_1$ plane to get the complete failure surface. The values of k, ℓ and m are then simply read from the plot. The disadvantage of this approach is that it requires a considerable number of tests on truly undisturbed material, many of which

must be performed at high pressures in order to determine the value of m. A second approach is to perform a sufficient number of plane strain tests to determine values for the cohesion, c, the angle of internal friction, ϕ, and the maximum shear strength, S_{max}, of the material. This method is made possible because, for plane strain, k, ℓ and m are functions of c, ϕ and S_{max}. The relationships among these six variables are given below.

$$k = \frac{3c}{\sqrt{(9 + 12 \tan^2 \phi)}} \tag{3.5}$$

$$\ell = S_{max} - k \tag{3.6}$$

$$m = -\frac{2\ell}{\alpha} \tag{3.7}$$

$$\alpha = \frac{\tan \phi}{\sqrt{(9 + 12 \tan^2 \phi)}} \tag{3.8}$$

In most cases it is sufficient to assume a value for S_{max} rather than trying to obtain a value from a series of tests. The only requirement on the value selected is that it gives a reasonable failure surface for the soil in the stress range (J_1) that will be considered.

Two elasto-plastic cases were considered, the difference between the two being the values selected for the strength parameters c, ϕ and S_{max}. These values are given in Table 3.2 and the resulting yield surfaces are shown in Fig. 3.6. If the yield criterion is satisfied, the stress state must

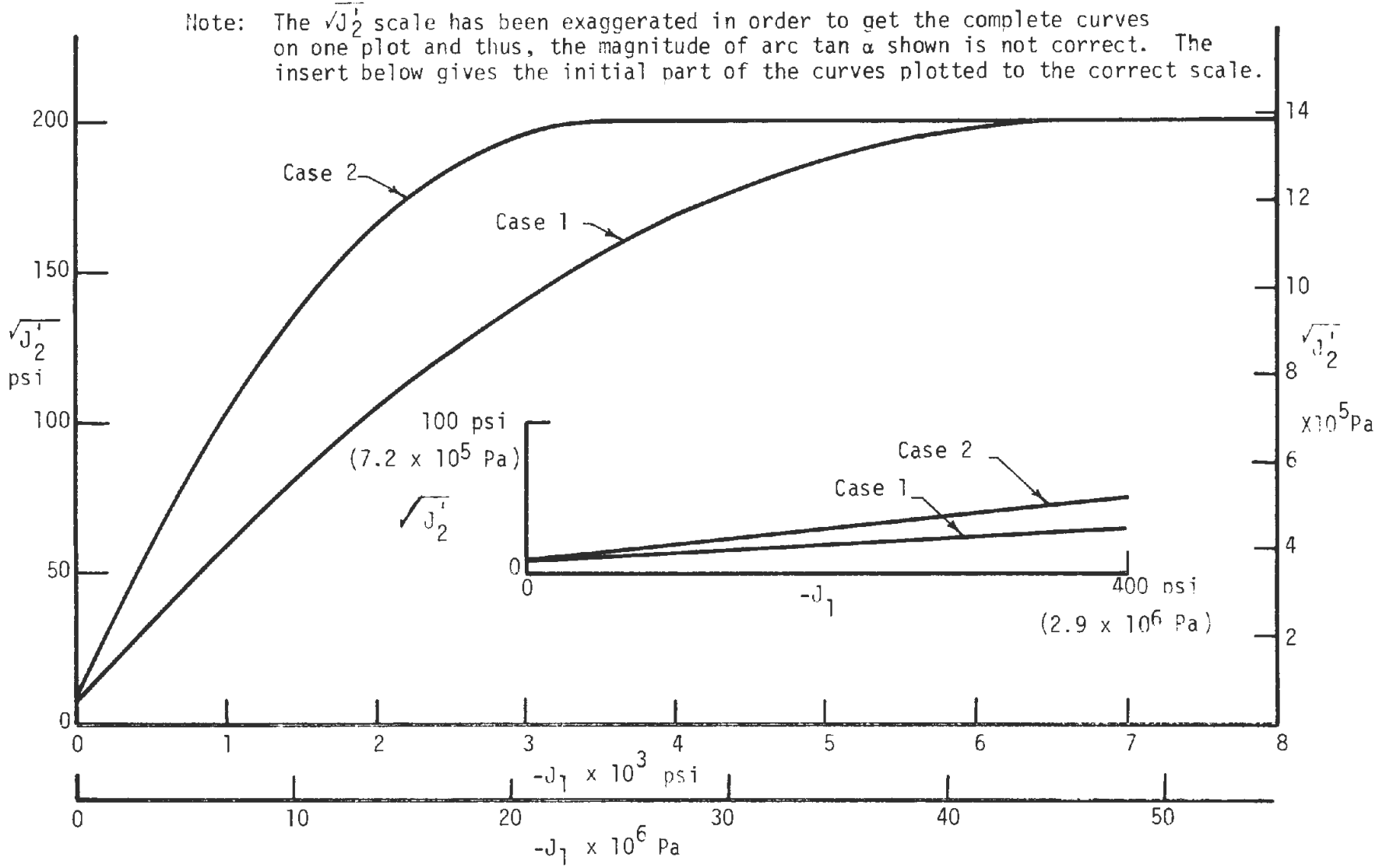

FIGURE 3.6 YIELD SURFACES SELECTED FOR THE TWO ELASTO-PLASTIC CASES

lie on the surface defined by f_1 in Eqs. 3.1 and 3.2 (Fig. 3.6). An element whose stress state plots below f_1 behaves elastically for that increment,

TABLE 3.2

STRENGTH PARAMETERS USED IN THE ELASTO-PLASTIC ANALYSES

	c psi (Pa)	ϕ degrees	S_{max} psi (Pa)	k psi (Pa)	ℓ psi (Pa)	m psi (Pa)
Case 1	7 (4.8×10^4)	10	200 (1.4×10^6)	6.9 (4.75×10^4)	193.1 (1.33×10^6)	-6710 (-4.6×10^7)
Case 2	8 (5.5×10^4)	20	200 (1.4×10^6)	7.4 (5.1×10^4)	192.6 (1.32×10^6)	-3445 (-2.4×10^7)

whereas an element whose stress state plots on the failure surface has yielded. Points above f_1 are not possible.

Eight steps were used for the elasto-plastic cases as follows:

Step 1: All elements were assigned the properties of soil and the dead load was applied to them.

Step 2: This was an equilibrium iteration.

Step 3: Those elements within the boundary of the exterior surface of the intended liner were deactivated (excavation) and those elements comprising the liner were activated (liner placement).

Steps 4-8: Same as step 2.

3.2.4 TIME-DEPENDENT MODEL

In this investigation two cases were considered using the viscoelastic or creep model. For material behavior of this type the total strain is defined to be the sum of instantaneous elastic and creep parts. The strain is also divided into deviatoric and volumetric components. Thus, it is possible to have either elastic or viscoelastic deviatoric deformation and to have either elastic or viscoelastic volumetric deformation. It is felt that a reasonably realistic model would consist of elastic volumetric deformation combined with viscoelastic deviatoric deformation. Thus, this was the combination used.

The viscoelastic deviatoric strain was defined by the Kelvin model which consists of a spring and a dashpot in parallel, and the strain-time relation for any time $t + \Delta t$ can be expressed as follows:

$$\gamma^c_{t+\Delta t} = \gamma^c_t \exp(-a_1 \Delta t) + \tau_t \frac{a_2}{a_1} [1 - \exp(-a_1 \Delta t)] \qquad (3.9)$$

where $a_1 = \frac{G}{\eta}$, $a_2 = \frac{1}{\eta}$, and G and η are the spring and the dashpot constants, in this case for shear, respectively. The superscript c indicates the creep strain component. (This is the incremental form of the relation used in the finite element program). When a stress is applied to an element at $t = 0$, the total elastic volumetric strain occurs instantaneously at $t = o$. At $t > o$ the additional viscoelastic deviatoric strain given by Eq. 3.9 begins and continues until equilibrium is reached and all creep ceases (theoretically at $t = \infty$). The total strain at any time is given by the sum of these two strain components.

The elastic constants used for the two time-dependent cases were the same as those used in the linear-elastic and elasto-plastic cases. The new variable introduced here was the viscous dashpot constant, η, which was given the value of 1.31×10^4 lb-hr/in^2 (3.25×10^{11} Pa-sec.). The resulting creep curve is given in the generalized non-dimensional form in Fig. 3.7. The effect of both loading and unloading are shown.

The material properties for the two time-dependent cases studied were the same. The difference between the two cases was the time of liner placement after excavation. In the first case the liner was installed simultaneously with the excavation step. This was identical to the procedure used in the time-independent linear-elastic and elasto-plastic analyses. For the second case a short time was allowed to elapse after excavation before the liner was installed.

The first step, during which the dead load was applied to a system composed entirely of soil elements, corresponded to time zero. Each succeeding step was designated to occur at a time greater than the previous step. In considering the soil-liner system to be modeled it was assumed that while the soil mass may have undergone creep in the past it had reached equilibrium prior to excavation. Thus, a series of steps was added after the dead load step to insure that all time-dependent deformation had ceased prior to the excavation step. The excavation and liner placement step(s), as described in the previous paragraph, followed. Since these operations imposed a stress change on the system a second series of steps was provided to allow enough time for all the creep to occur.

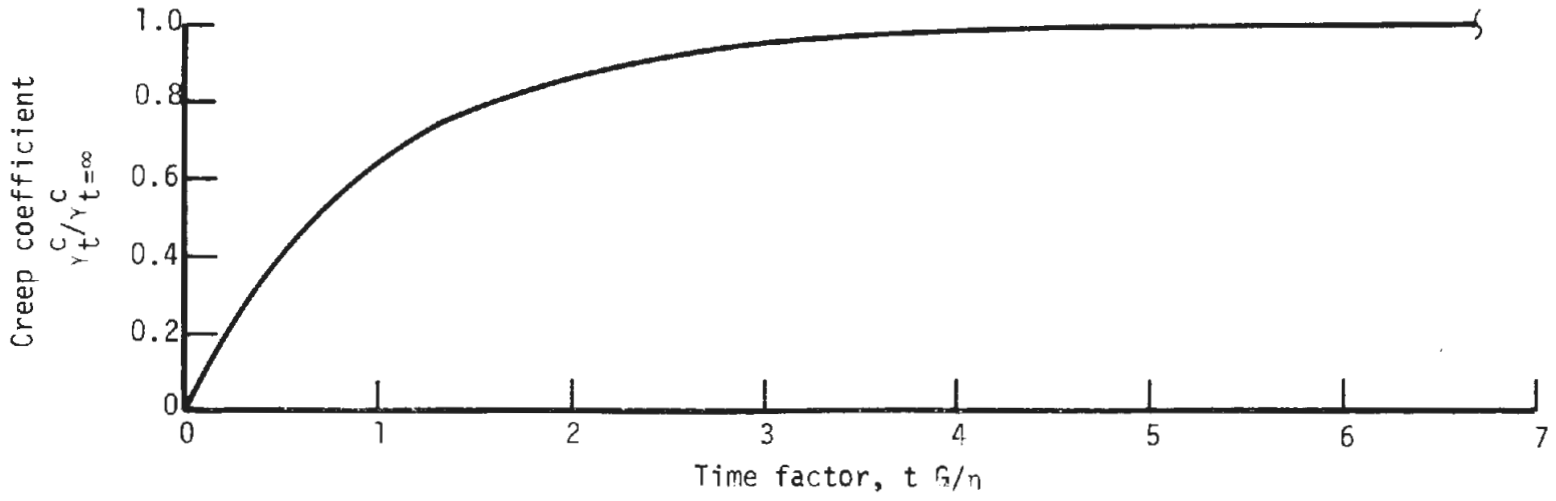

a. Loading curve

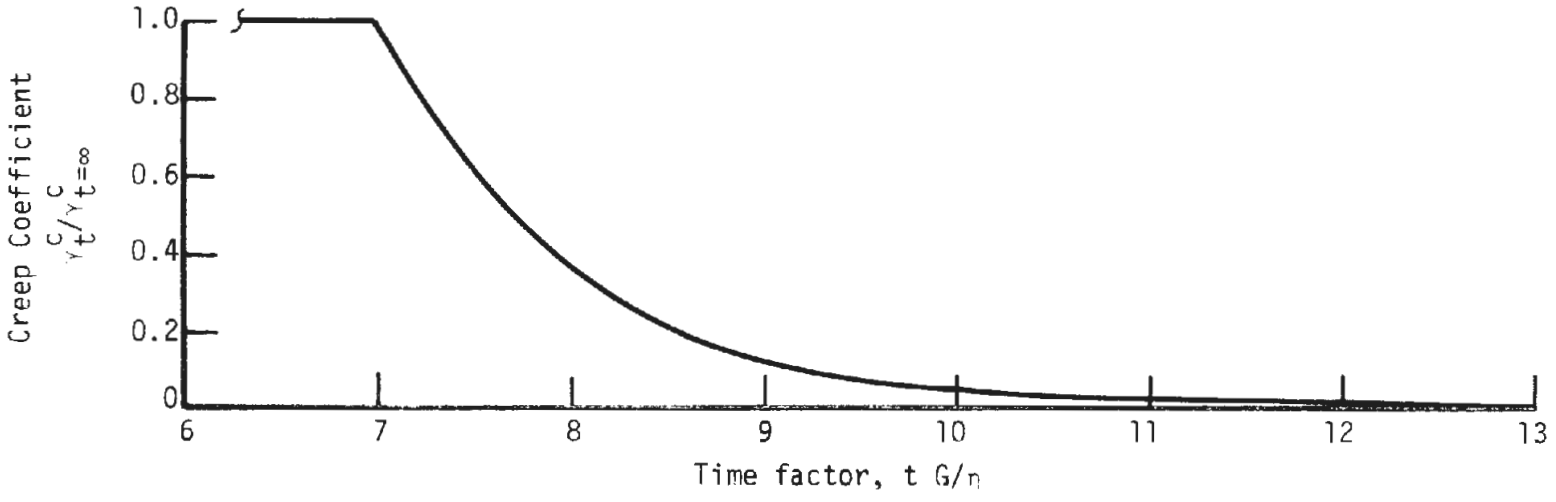

b. Unloading curve

FIGURE 3.7 CREEP CURVES SELECTED FOR THE TIME-DEPENDENT ANALYSES

3.3 RESULTS OF ANALYSIS

3.3.1 GENERAL

The output data supplied by the finite element program consists of the stresses and strains for each element and the displacements of each node. These quantities are referenced to the x-y coordinate system where x is the horizontal direction in Fig. 3.2 and y is the vertical direction.

For each of the cases investigated the "liner" element stresses were used to calculate the thrust, shear and moment distributions around the liner. The stresses in the "soil" elements immediately surrounding the liner were used to calculate the radial and shear stresses acting on the liner. The force and stress distributions are given for each case in Sections 3.3.2 and 3.3.4.

3.3.2 ANALYSIS OF A TUNNEL IN A LINEAR-ELASTIC MEDIUM

The results from the one case in which linear-elastic material behavior was considered are presented in Figs. 3.8 and 3.10. Figure 3.8 gives the initial and final distributions of radial normal stresses and tangential shear stresses acting on the liner. Displacements of the liner and the ground surface are given in Fig. 3.9. The resulting thrust, shear and moment distributions are given in Fig. 3.10.

The analysis was based on the assumption that the tunnel was excavated and the liner installed instantaneously. Under these conditions the surrounding medium remains undisturbed and the original stresses acting in

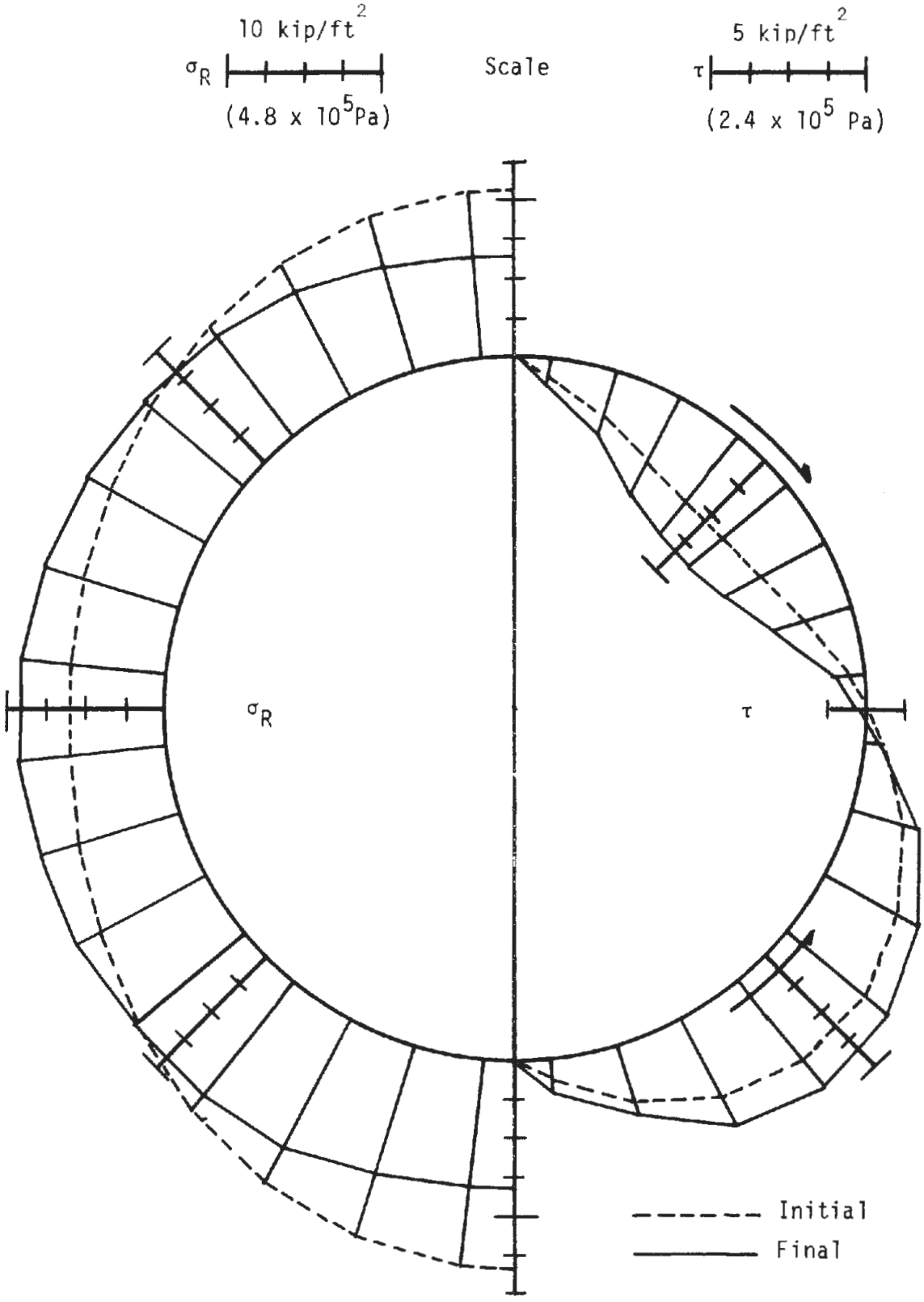

FIGURE 3.8 INITIAL AND FINAL DISTRIBUTIONS OF EXTERNAL STRESSES ACTING ON THE LINER--LINEAR-ELASTIC CASE

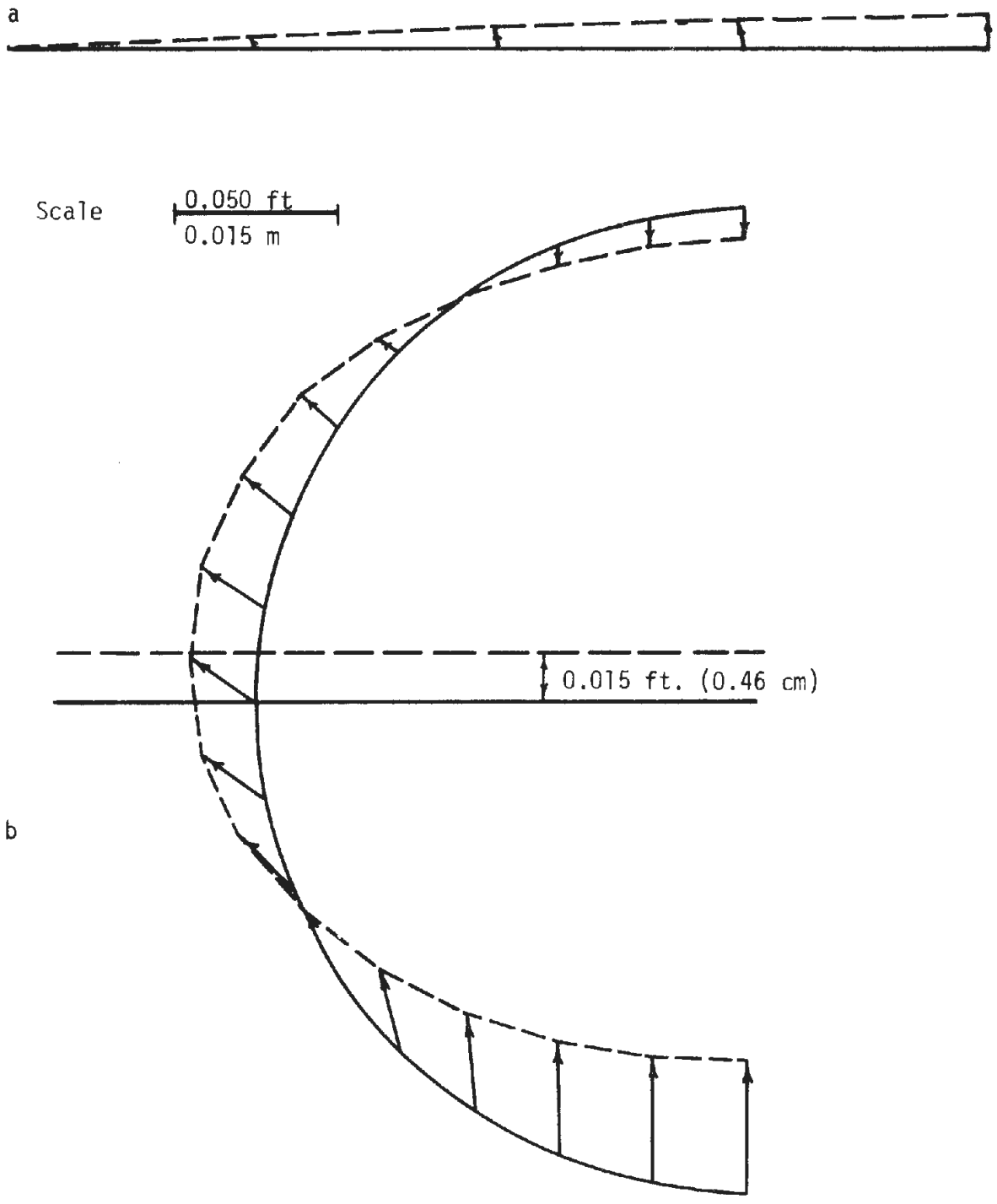

FIGURE 3.9 DISPLACEMENTS OF THE LINER AND GROUND SURFACE--LINEAR-ELASTIC CASE

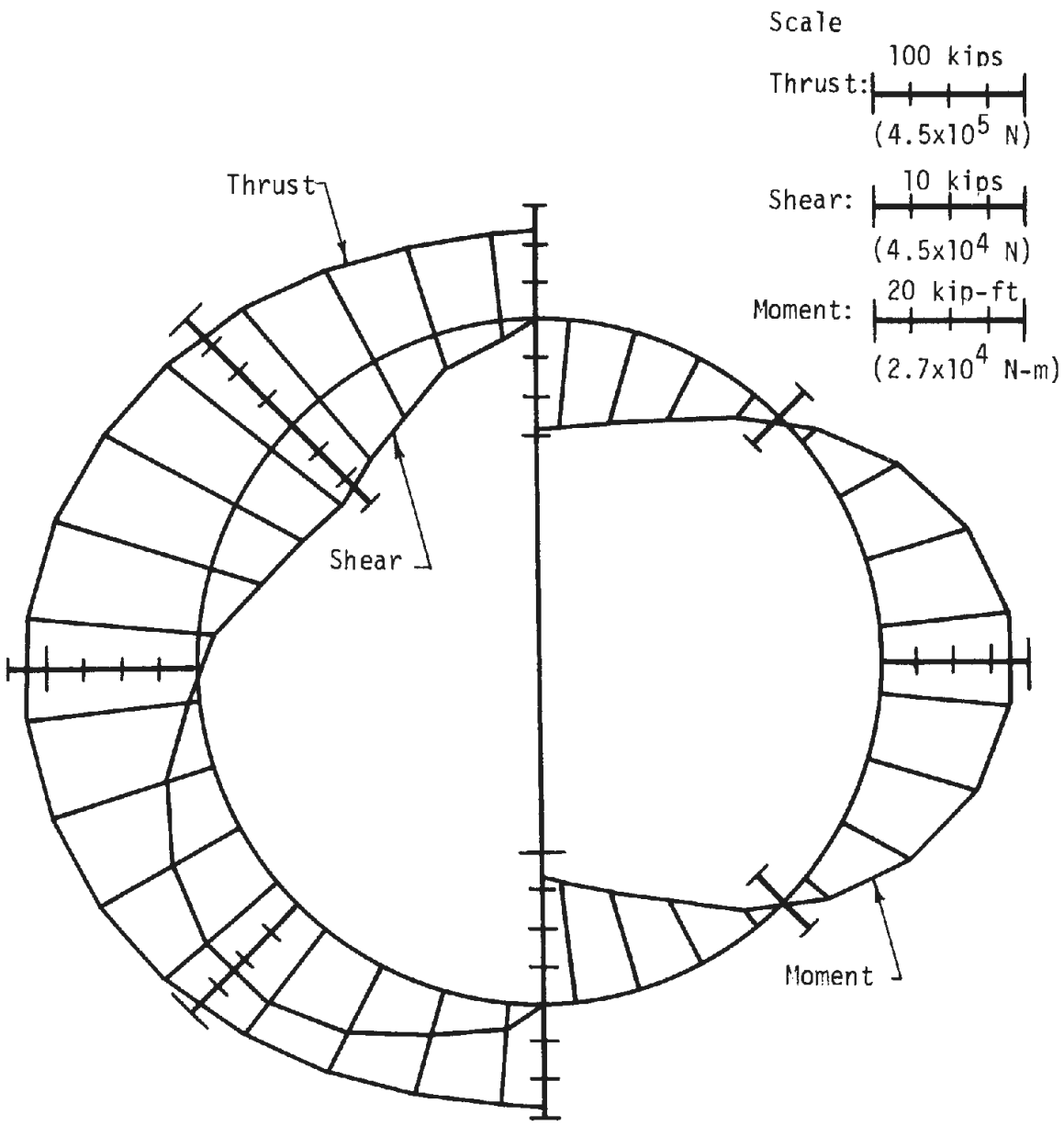

FIGURE 3.10 THRUST, SHEAR AND MOMENT DISTRIBUTIONS CALCULATED FOR THE LINEAR-ELASTIC CASE

the medium come to bear on the liner without reduction. The medium stresses are not altered until the liner begins to deform. Strictly speaking this is not a realistic assumption because it is known that some deformations and disturbance does occur before a liner can be placed, thus reducing the external pressure that will initially act on the liner.

A value of 0.5 was selected for K_o, the coefficient of earth pressure at rest, which is the ratio of horizontal to vertical stress. As can be seen from the dashed curve for σ_R in Fig. 3.8, this gives initial radial stresses at the crown and invert which are approximately twice the stress at the springline. The relationship is not exact because of the increase in stress with depth.

Since the liner is deformable it is forced to deform by these external pressures (Fig. 3.9). It assumes an ellipsoidal shape as the crown and invert move inward and the springline is forced outward. These deformations in turn have an influence on the applied pressures. As the crown and invert move inward the radial pressure in these areas is reduced. As the springline moves outward against the soil the pressure there is increased. Thus the final radial stress distribution is given by the solid curve in Fig. 3.8. In addition, as the liner deforms it tries to slip past the adjacent soil. However, since this slip has been restricted in this analysis, the shear stress increases in magnitude as shown by the curves to the right in Fig. 3.8.

Fig. 3.10 gives the distributions of thrust, shear and moment calculated from the internal liner stresses. The forces appear reasonable

and about what would be predicted from consideration of the external pressure distributions. Indications are that the external shear stresses contribute significantly to the magnitude of the internal forces in this case. It can be seen in Fig. 3.8 that the final external radial stresses are slightly larger at the springline than at the crown and invert. On the basis of these stresses alone it would be expected that the thrust would be greater at the crown and invert than at the springline. Figure 3.10 shows, however, that this is not the case. The difference between predicted and observed thrusts is due to the action of the external shear stresses. They "drag" on the liner, as indicated by the two "arrows" in Fig. 3.8, such as to increase the thrust at the springline and reduce it at the crown and invert. Determination of the relative influence of the two external stresses on the moment distribution is a complex procedure. In general, it can be said that they counteract each other and if there were no external shear the absolute magnitude of the moments would be reduced at the springline and increased at the crown and invert.

Figure 3.9b shows that the deformed shape of the liner is that of an ellipse, the horizontal axis of which is slightly above the axis of the originally circular liner. Figure 3.9a shows that the ground surface was displaced upwards a small amount. This upward displacement was the result of the elastic behavior of the medium. This would not be expected to occur over an actual tunnel unless the tunnel was driven in a material that behaved elastically and that did not tend to collapse in the crown. In real tunnels in very stiff clay (so strong that it remains elastic even near the tunnel) the ground surface has been observed to rise.

3.3.3 ANALYSIS OF A TUNNEL IN AN ELASTO-PLASTIC MEDIUM

The results obtained for the two cases in which elasto-plastic material behavior was considered are presented in Figs. 3.11 through 3.16.

In these analyses the combination of ϕ and K_o used was such that when the dead load was applied to the system, the stress difference, σ_v-σ_h, below a certain depth was large enough to cause yielding. The resulting redistribution of stresses altered the value of K_o in the yielded zones. Figure 3.11 shows the extent of initial yielding and the new K_o values as a function of depth for the two cases. Since case 2 was the one with the higher ϕ value, its critical depth was greater than that for case 1 and the amount of stress redistribution, or K_o alteration, was less. For case 1 the K_o value was increased from 0.50 to approximately 0.65 in the area around the tunnel. For case 2 the initial yielding occurred below the tunnel and the K_o value around the tunnel remained 0.50.

The initial and final distributions of external stresses acting on the liner for elasto-plastic cases 1 and 2 are shown in Fig. 3.12 and 3.13 respectively. Due to the increased K_o the resulting initial radial stress distribution for case 1 is slightly more uniform around the liner than that in the linear-elastic case where $K_o = 0.5$. Also, the larger K_o meant that the stress difference, $\sigma_v - \sigma_h$, was smaller and thus, the magnitude of the initial external shear stresses was decreased. Compare Fig. 3.12 and 3.8. Since the elasto-plastic case 2 had the same effective K_o around the liner as the linear-elastic case there was essentially no difference in the initial external stress distributions for these two cases.

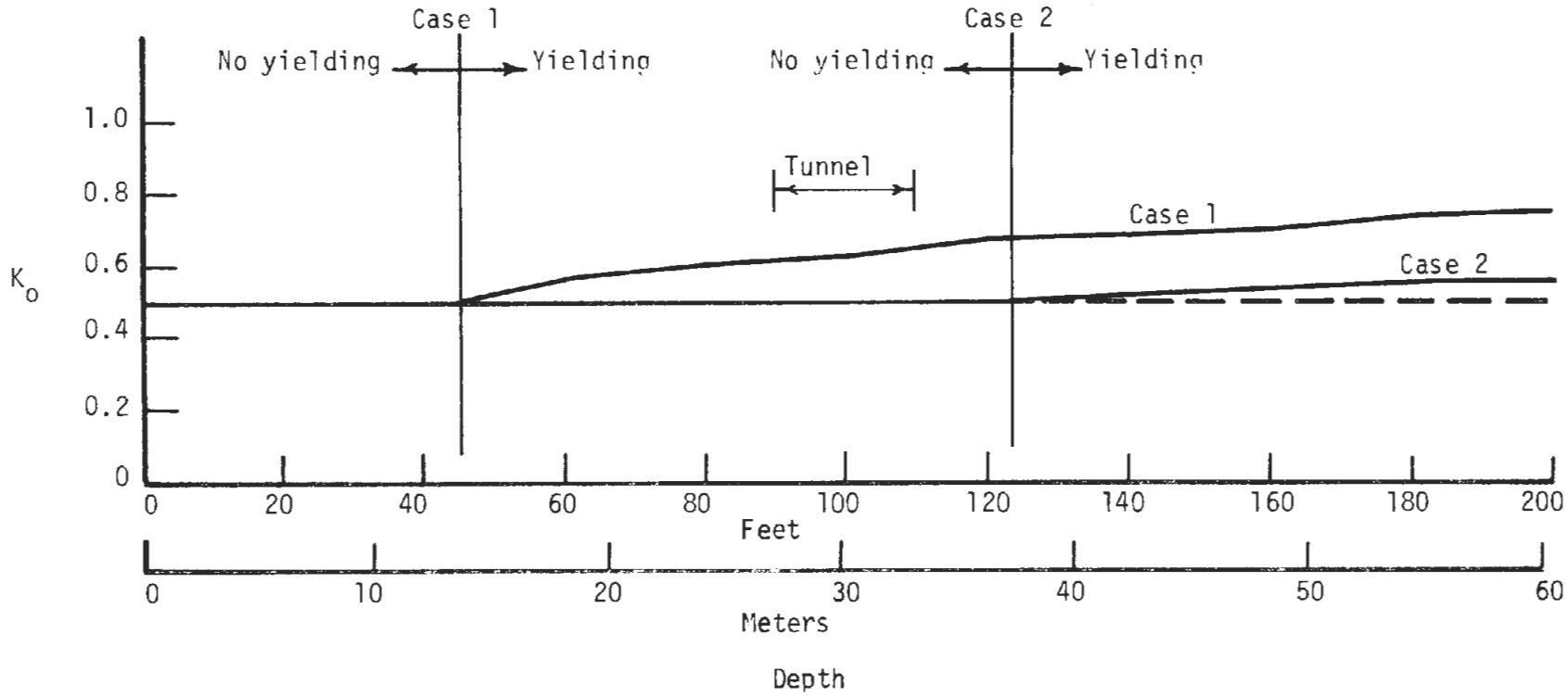

FIGURE 3.11 VARIATION OF K_o WITH DEPTH--FIRST LOAD STEP--ELASTO-PLASTIC CASES 1 AND 2

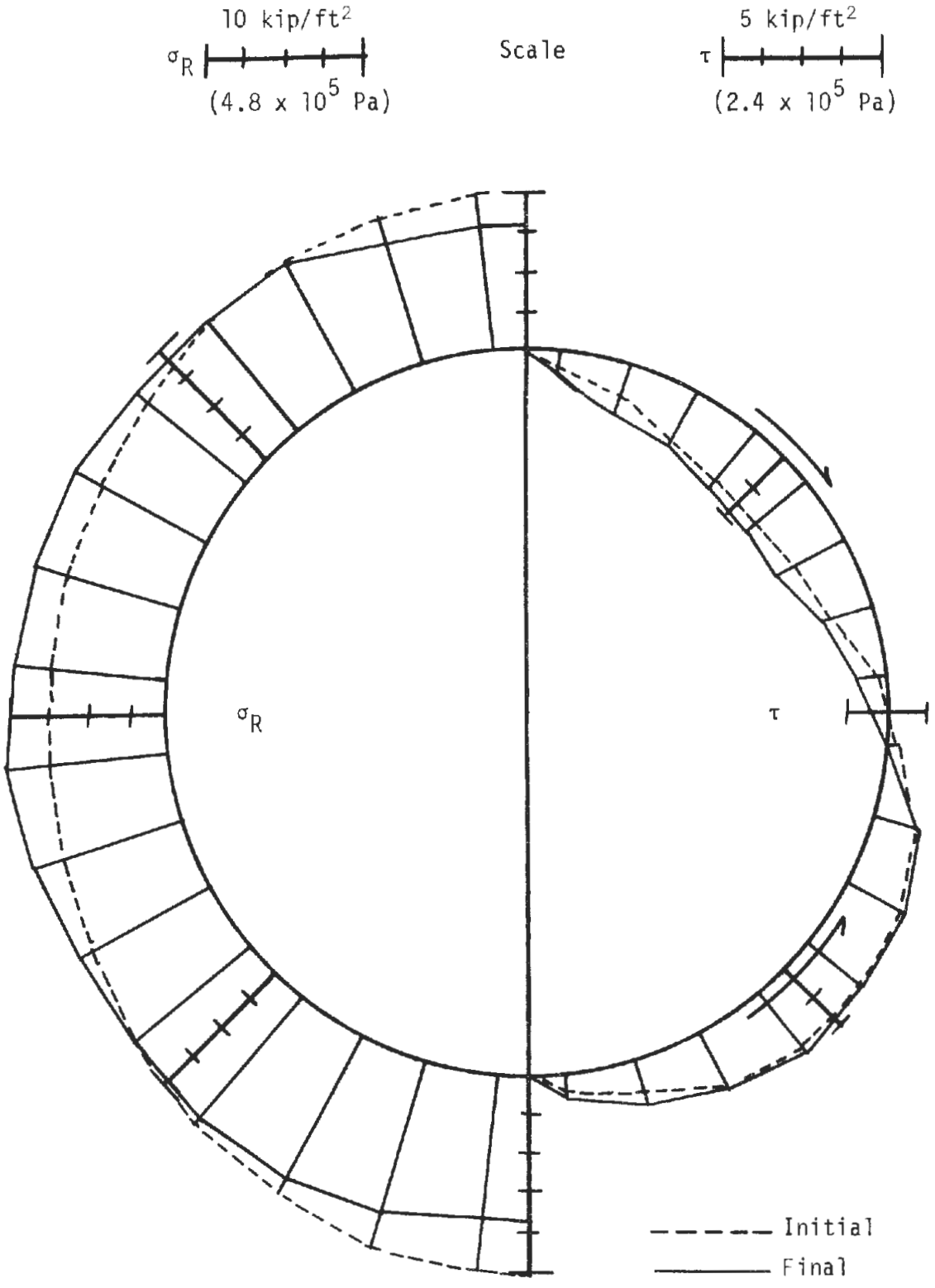

FIGURE 3.12 INITIAL AND FINAL DISTRIBUTIONS OF EXTERNAL STRESSES ACTING ON THE LINER--ELASTO-PLASTIC CASE 1

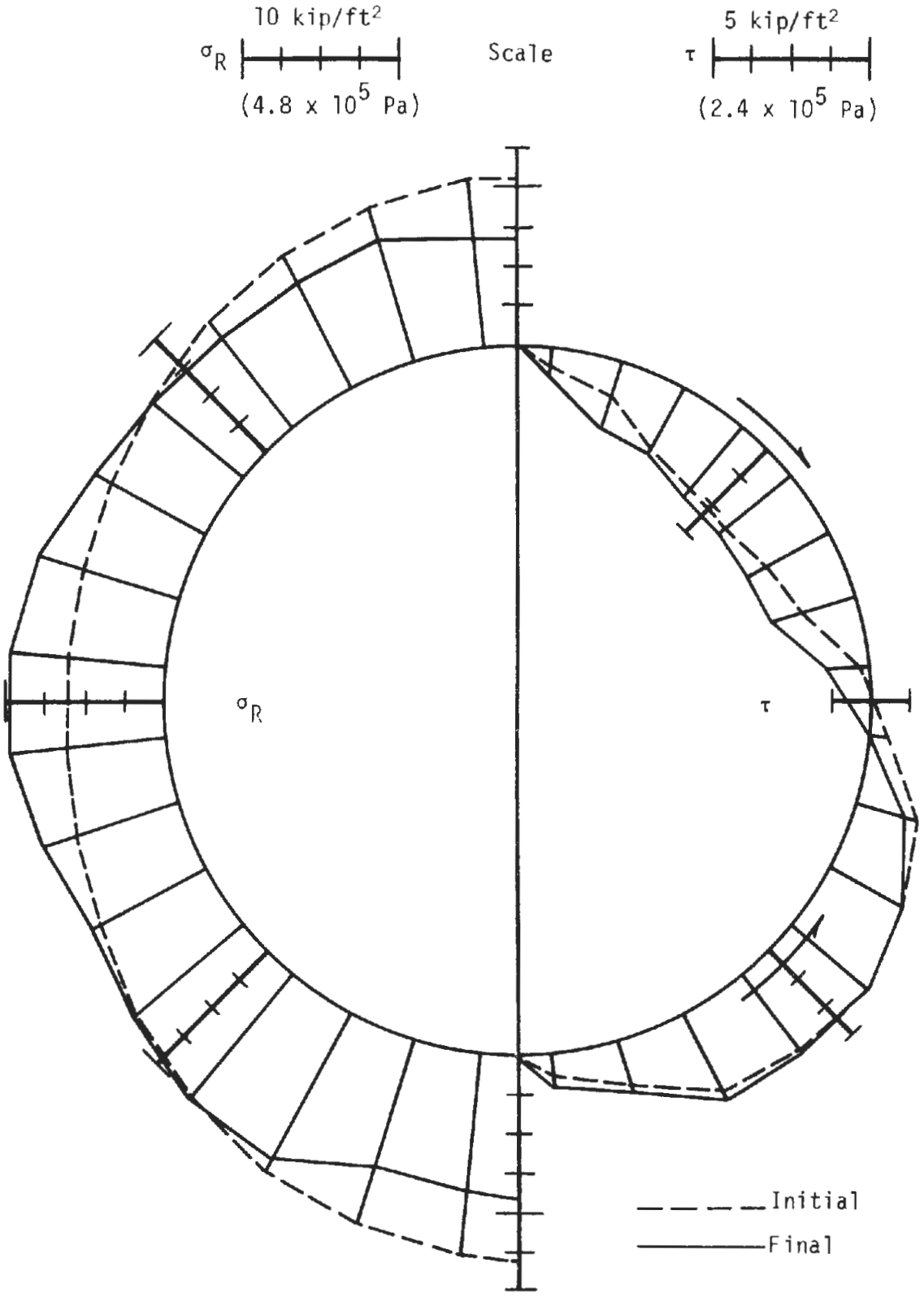

FIGURE 3.13 INITIAL AND FINAL DISTRIBUTIONS OF EXTERNAL STRESSES ACTING ON THE LINER--ELASTO-PLASTIC CASE 2

When the tunnel was excavated and the liner installed the equilibruim of the system was disturbed. The resulting deformations and stress changes caused additional yielding. Those elements that yielded for each of cases 1 and 2 are shown by the horizontally and vertically cross-hatched regions, respectively, in Fig. 3.14.

Yielding occurs in areas of high shear stress, or in other words, in areas where the stress difference is large. Considering this, the position of the yielded zones around the liner in Fig. 3.14 are as would be expected. As the liner deformed under load the vertical stresses were reduced at the crown and invert and the horizontal stresses were increased at the springline. Since initially the vertical stress was larger than the horizontal stress these changes resulted in a reduction of the stress differences at the crown, invert and springline. Thus, the chances of yielding occurring in these areas were diminished. Simultaneously with these stress changes, the soil deformations, shown by the arrows in Fig. 3.14, were acting to increase the shear stress in the zones approximately 45 degrees from the vertical, thus increasing the likelihood of yielding there.

In these two cases the strength properties of the soil were such that yielding did occur in zones approximately 45 degrees from the vertical. Since the soil in case 2 was of a higher strength than that in case 1, the yielding in case 2 was less extensive than in case 1, especially above the tunnel where the stresses were lower. Had the soil been assigned a high enough strength, no yielding would have occurred at all, given the stress changes that resulted here. Conversely, had the soil been of lower strength

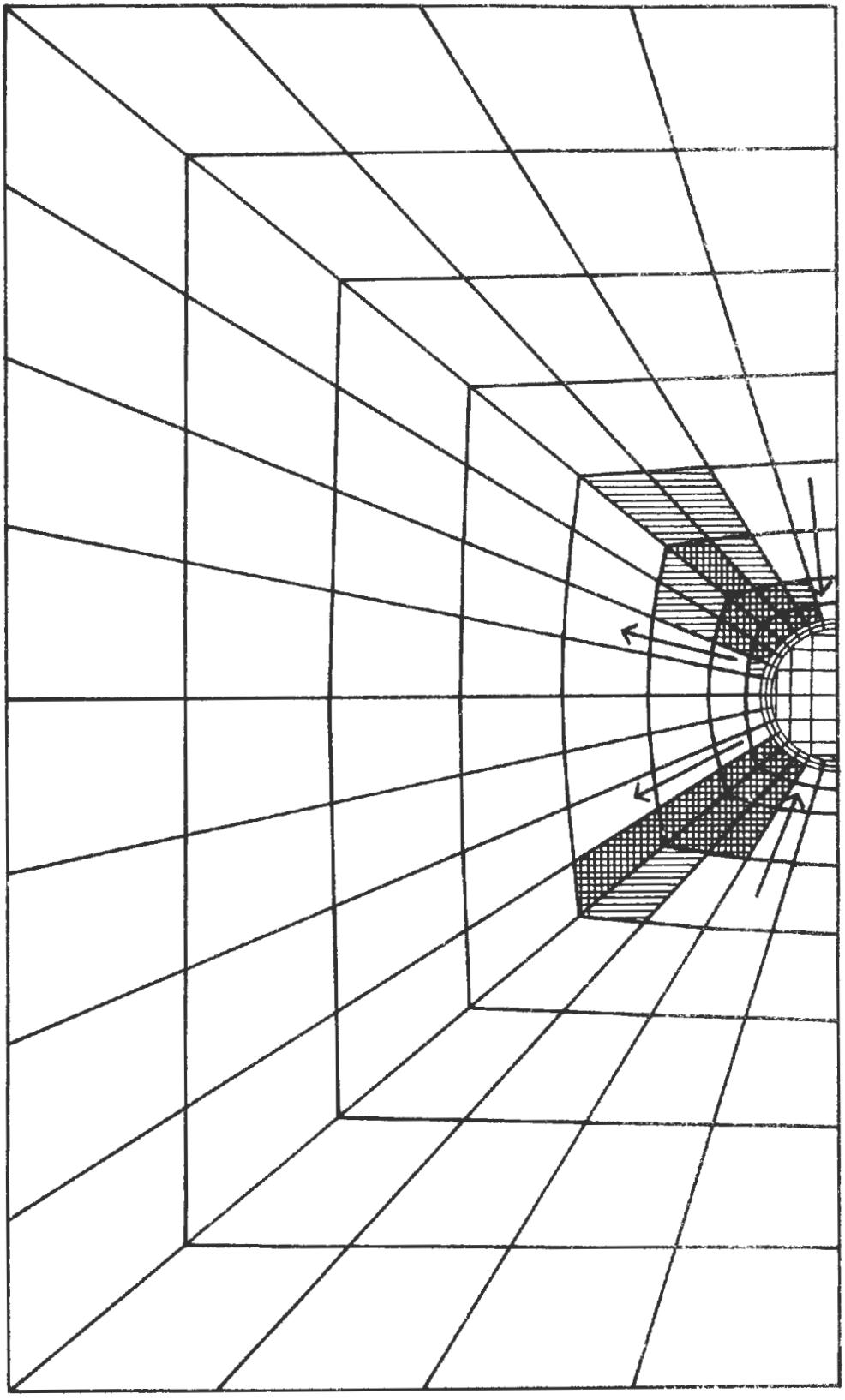

FIGURE 3.14 ZONES OF YIELDING AROUND LINER--ELASTO-PLASTIC CASES 1 (HORIZONTAL HATCHING) AND 2 (VERTICAL HATCHING)

the yielding would have been more widespread, approaching the crown, invert and springline.

The solid curves in Fig. 3.12 indicate the final distribution of external stresses acting on the liner for case 1. As in the linear-elastic case, deformation of the liner reduced the external radial stresses at the crown and invert while increasing them at the springline. However, since the stress distribution was initially more uniform (K_o = 0.65), the percent change is less here than in the linear-elastic case. The yielding that occurred after liner installation has had no apparent effect on the external radial stresses. However, it is obvious from Fig. 3.12 that there was much less change in external shear stresses in going from the initial to final states than was observed for the linear-elastic case. There was an increase in magnitude, but it was very slight. The increase was the smallest at those locations where it was the greatest in the linear-elastic case. This was a result of the yielding. When an element yields, the stress difference, and thus the shear, in that element is reduced from what it would have been if no yielding occurred. In this case the zones of yielding (Fig. 3.13) coincided with the locations of the maximum external shear. Thus, the increased shear stresses that normally would have built up were instead dissipated by the yielding.

Except for the influence of an altered K_o, observations similar to those in the preceeding paragraph can be made for case 2 which represents a somewhat higher strength soil. There is very little difference between the final radial stress distribution for this case and the distribution

obtained for the linear-elastic case. Again the shear stresses have been reduced by yielding, especially on the lower half of the liner.

Figure 3.15 and 3.16 show the distributions of thrust and shear forces and bending moments areound the liner for cases 1 and 2 respectively.

Comparing case 1 with the linear case, the following observations can be made. First, thrust at the crown and invert is greater in case 1 than in the linear-elastic case. This results because the case 1 liner is subjected to larger external radial stresses and smaller external shear stresses than the liner for the linear-elastic case. For the same reason the springline thrust in both cases is about the same. The difference in external stresses between the two cases also accounts for the differences in moment distributions. By comparing Figs. 3.10 and 3.15 it can be seen that there is very little difference in moments at the crown, springline and invert. Rather, the differences occur at points between these locations (corresponding to the yield zones), where the magnitudes of the moments are greater for the elasto-plastic case.

Shear forces in the liner are related to the moment distribution. Had the bending moments been of constant magnitude (and same sign) around the liner there would have been no shear forces. In other words, the more uniform the moment distribution, the lower are the magnitudes of the shear forces. In addition, a change of slope of the moment curve results in a change of sign of the shear forces. Considering these facts, the differences between shear force distributions for the linear-elastic case and case 1 are due to the differences in the moment distributions of the two cases.

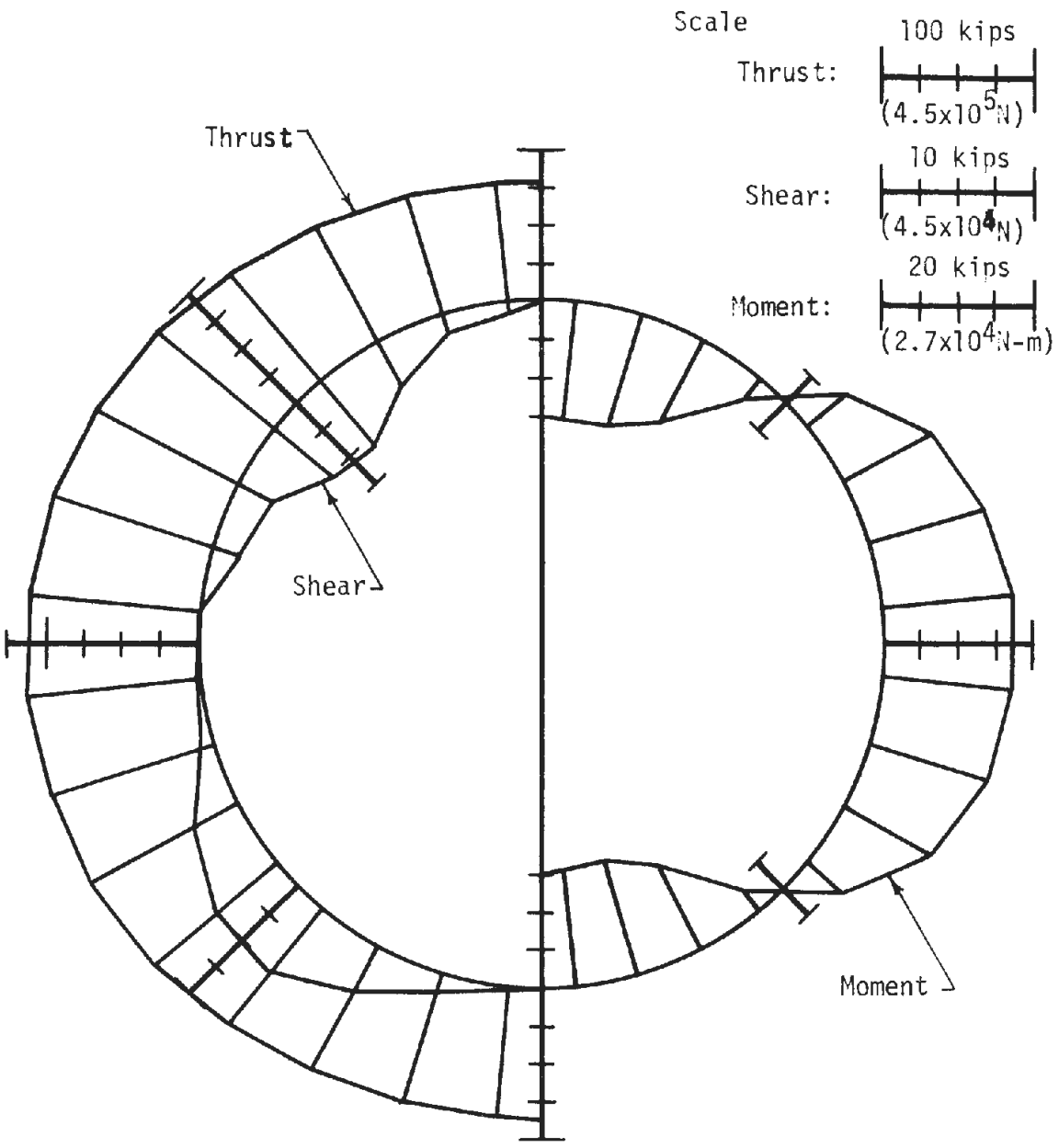

FIGURE 3.15 THRUST, SHEAR AND MOMENT DISTRIBUTIONS CALCULATED FOR ELASTO-PLASTIC CASE 1

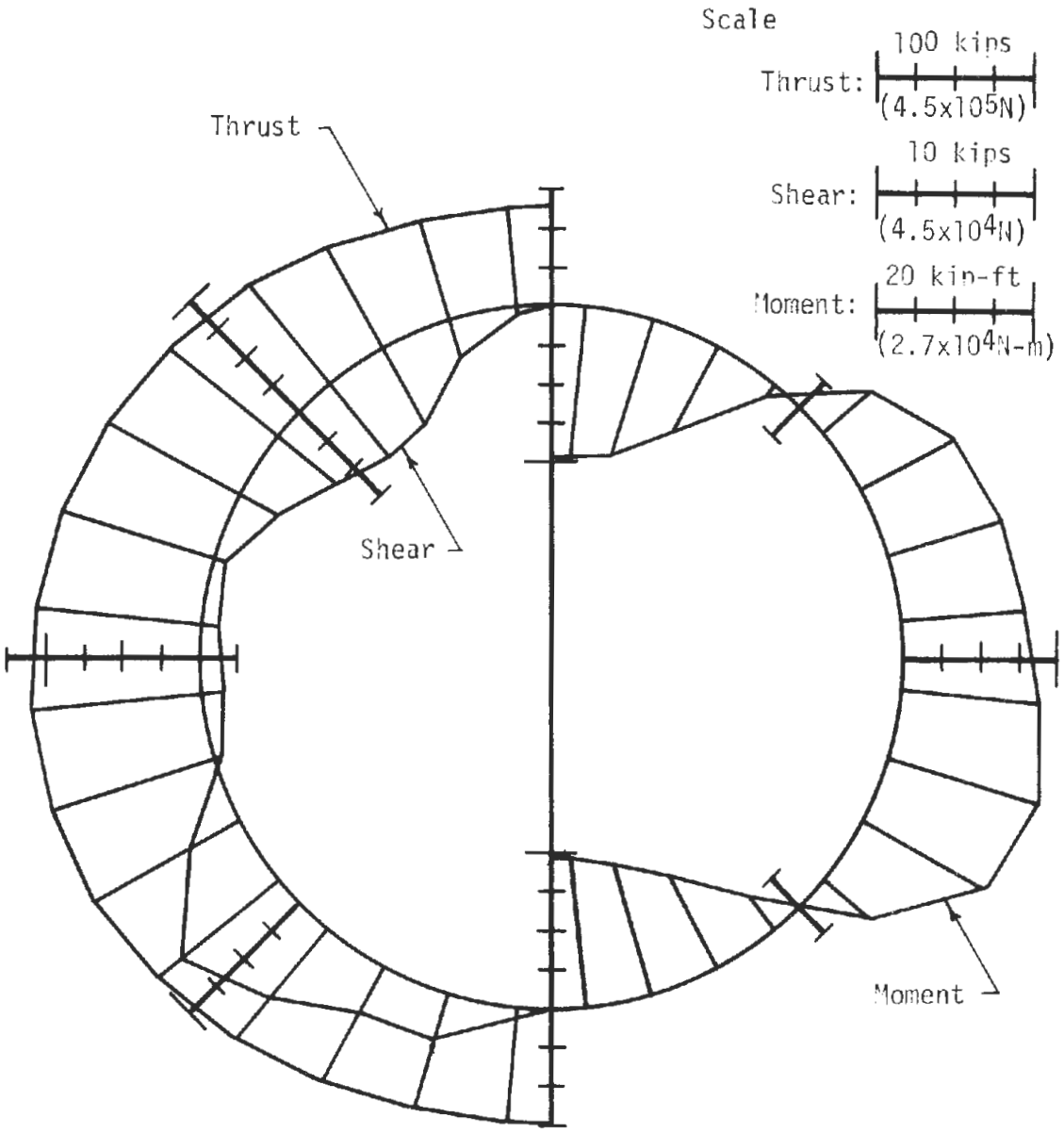

FIGURE 3.16 THRUST, SHEAR AND MOMENT DISTRIBUTIONS CALCULATED FOR ELASTO-PLASTIC CASE 2

Differences between the force and moment distributions for the elasto-plastic case 2 and the linear-elastic case can be explained in the same manner as for the above case 1, except that, here there is no K_o difference to cloud the issue. It appears that the variations between the external shear distributions that resulted for the two models had the most influence on the differences between liner forces for the two cases. The thrust distributions for the two cases were very similar. The thrusts were just slightly higher at the crown and invert and slightly lower at the springline for the elasto-plastic case 2. The negative bending moments at the crown and invert were significantly larger in case 2.

For the three cases considered to this point it appears that, because of the instantaneous installation of the liner, the non-linear analysis has provided very little new information that could not have been obtained from the linear-elastic analysis. The most significant differences were in the distributions of bending moments, which indicates that the linear-elastic analysis underestimates the moments at locations away from the springlines, although maximum values were about the same. It cannot be concluded, however, that these relative results will carry over and be generally applicable to all cases. The range of material properties considered here is too small to make any general conclusions from the results.

3.4.4 ANALYSIS OF A TUNNEL IN A CREEPING MEDIUM

The results obtained for the two cases in which time-dependent material behavior was considered are presented in Figs. 3.17 through 3.20.

In these two cases, creeping of the medium was initiated upon application of the dead load. As explained in Section 3.2.4 this initial creep was allowed to dissipate before excavation and liner installation. As creep occurred the stress state throughout the medium was altered, resulting in a reduction of the stress difference at each point. Vertical stresses, corresponding to the weight of the overburden, remained unchanged while the horizontal stresses increased. This caused an increase in K_o from an original value of 0.50 to approximately 0.80 throughout the medium.

The distribution of external stresses acting on the liner at various times for time-dependent cases 1 and 2 are shown in Figs. 3.17 and 3.18 respectively. For case 1 excavation and liner placement occurred simultaneously. For case 2 liner installation occurred a short time after excavation. The time interval corresponded to a change in time factor (tG/η, Fig. 3.7) of 0.043.

For both cases the curves labeled "initial" correspond to the distribution of stresses acting on a cylinder of soil just before it was excavated and replaced by the liner. These initial stress distributions were essentially identical for both cases because the material properties and the stress conditions in the surrounding soil were initially the same for the two cases.

Compared to the linear-elastic case, the time-dependent properties gave substantially larger initial radial stresses at the springline but about the same radial stresses at the crown and invert. "Initial" shear stresses were much smaller in the time-dependent cases than in the elastic case.

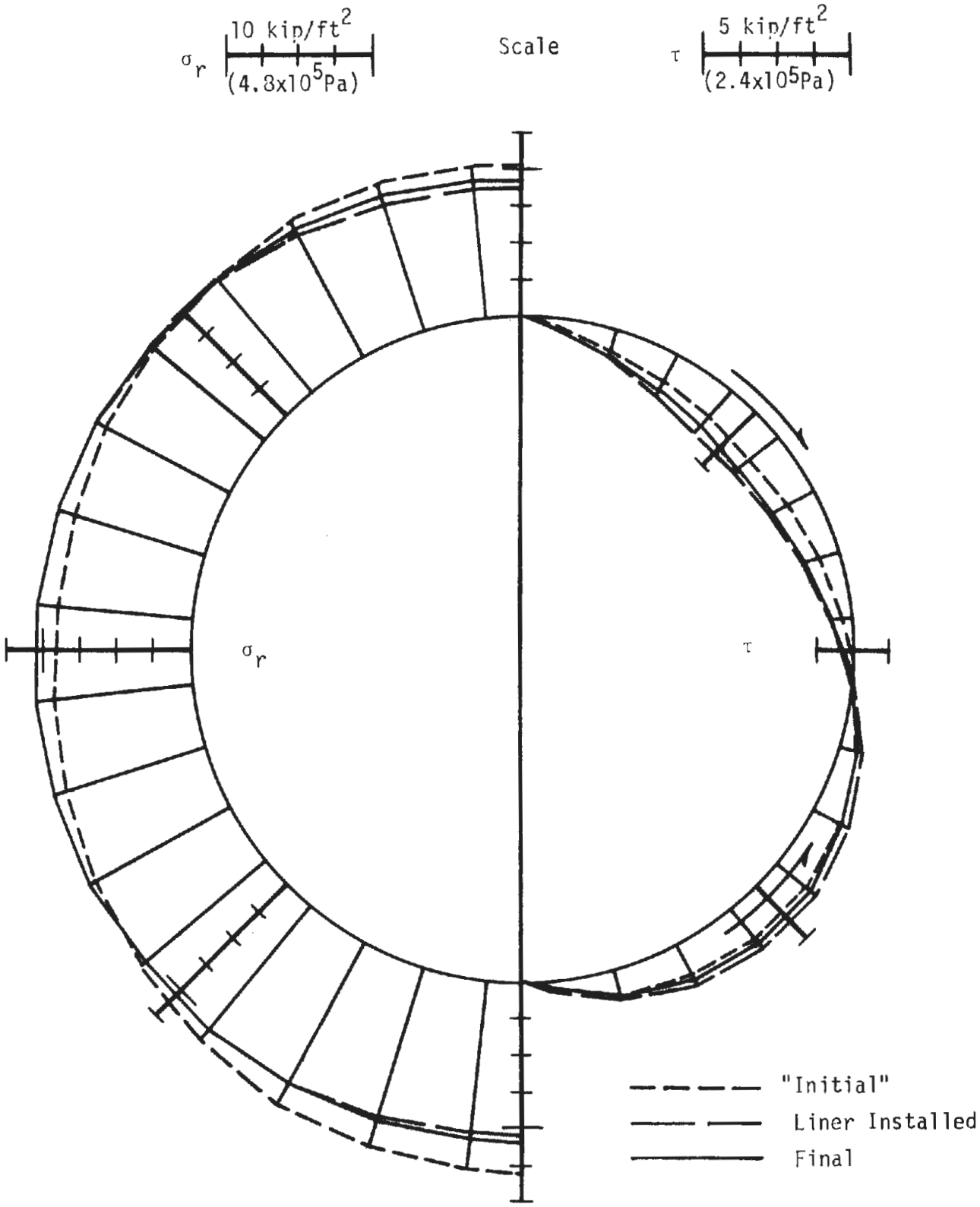

FIGURE 3.17 DISTRIBUTIONS OF EXTERNAL STRESSES ACTING ON THE LINER--TIME-DEPENDENT CASE 1

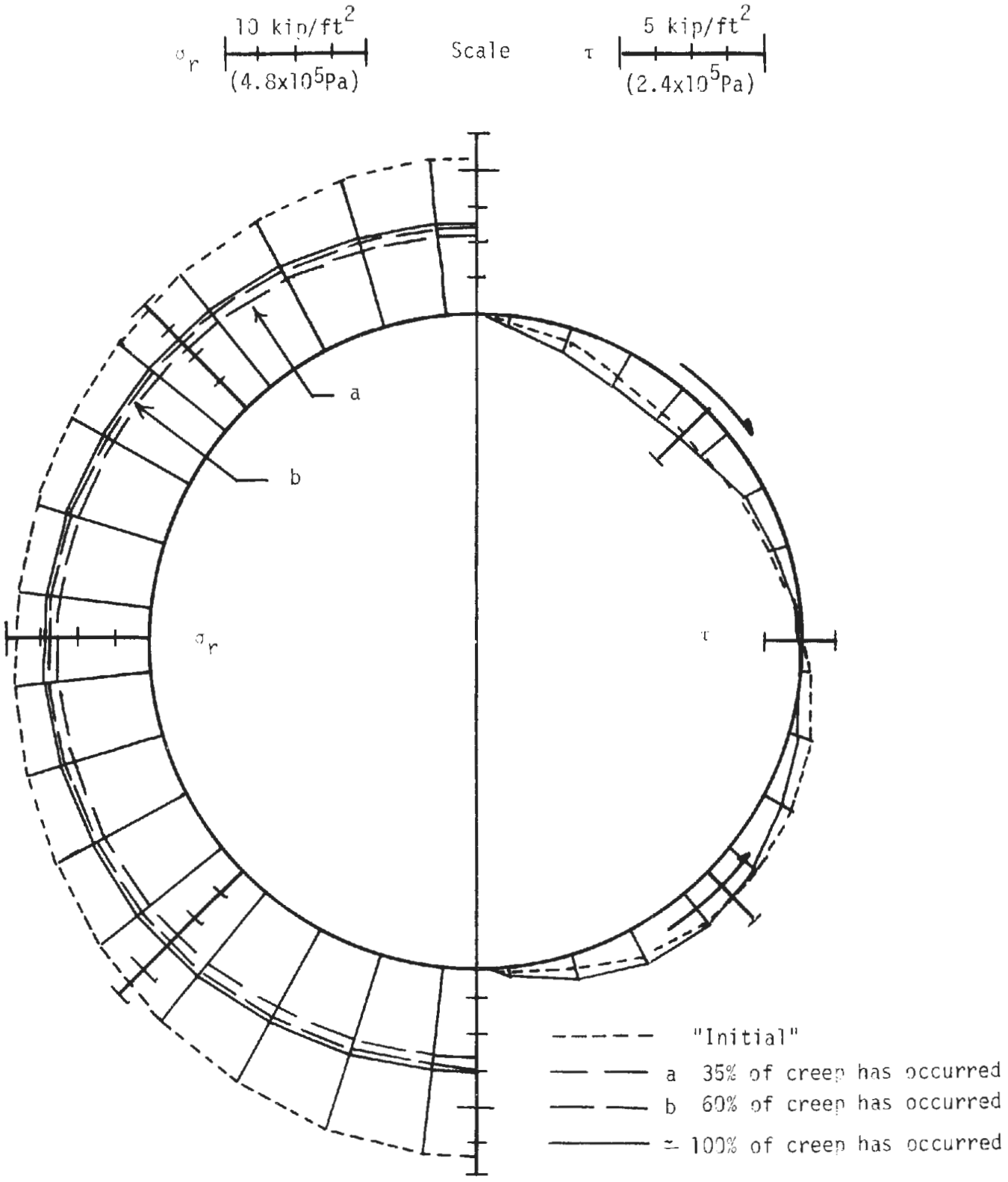

FIGURE 3.13 DISTRIBUTIONS OF EXTERNAL STRESSES ACTING ON THE LINER--TIME-DEPENDENT CASE 2

These differences were a result of the dead-load induced creep that occurred in the time-dependent cases. This creep had no effect on the vertical stresses in the soil, thus, there was little change in radial stresses at the crown and invert. The horizontal stresses in the soil were substantially increased by the creep effect, thus increasing the radial stresses at the springline. The "initial" shear stresses acting on the liner were less than in the linear-elastic case because the dead-load induced creep reduced the stress difference, $\sigma_v - \sigma_h$, and thus the shear stress.

Because the liner was installed instantaneously upon excavation and because the initial stress difference was small ($K_o = 0.80$) there was little change in the external stress distribution for time-dependent case 1. Immediately upon installation of the liner the external stresses, indicated by the dashed curves in Fig. 3.17, came to bear on it. The liner deformed causing a redistribution of stresses in the soil. This was entirely an elastic process since there had been no time for creep to occur. The external stresses at this point are given by the broken curves. With creep a further redistribution of stresses occurred. The final distribution of external stresses are given by the solid curves.

In case 2 the tunnel was excavated and for a short time interval there was no liner in place. During this time interval all of the elastic deformations and some negligible creep deformation occurred and the stresses on the tunnel boundary were zero. Therefore, at the instant the liner was placed there were no stresses acting on it. However, as time passed and

creep occurred in the soil external stresses on the liner were gradually built up. In Fig. 3.18 the broken curves a and b and the solid curve indicate the distribution of external radial stresses after 35, 60 and approximately 100 percent of the creep had occurred respectively. Only the final distribution of external shear stresses is shown because there was very little change with creep.

The distributions of thrust and shear forces and bending moments for time-dependent cases 1 and 2 are given in Figs. 3.19 and 3.20 respectively.

In Fig. 3.19 the curves labeled "a" correspond to the broken curves in Fig. 3.17 and the curves labeled "b" correspond to the final distribution of external stresses in Fig. 3.17. The curves "a" give the distribution of thrust, bending moment and shear due to elastic behavior only. Thus, these distributions can be compared to those for the linear-elastic case (Fig. 3.10). The differences observed can be attributed to the difference in K_o for the two cases. The difference between curves a and b indicate the effect of creep behavior for this case. There was a slight increase with time (creep) in thrust at the crown and invert, while there was no change at the springline. Considering the manner in which the external radial and shear stresses each contribute to the thrust distribution, it appears that the thrust was influenced more by the changes in shear stresses than by the changes in radial stresses. Apparently, thrust is not very sensitive to small changes in the external stresses. On the other hand, bending moments appear to be very sensitive to changes in the external stresses. Figure 3.19 shows that the moments were increased by almost 100 percent due to the same changes in external stresses that had almost no effect on the thrust.

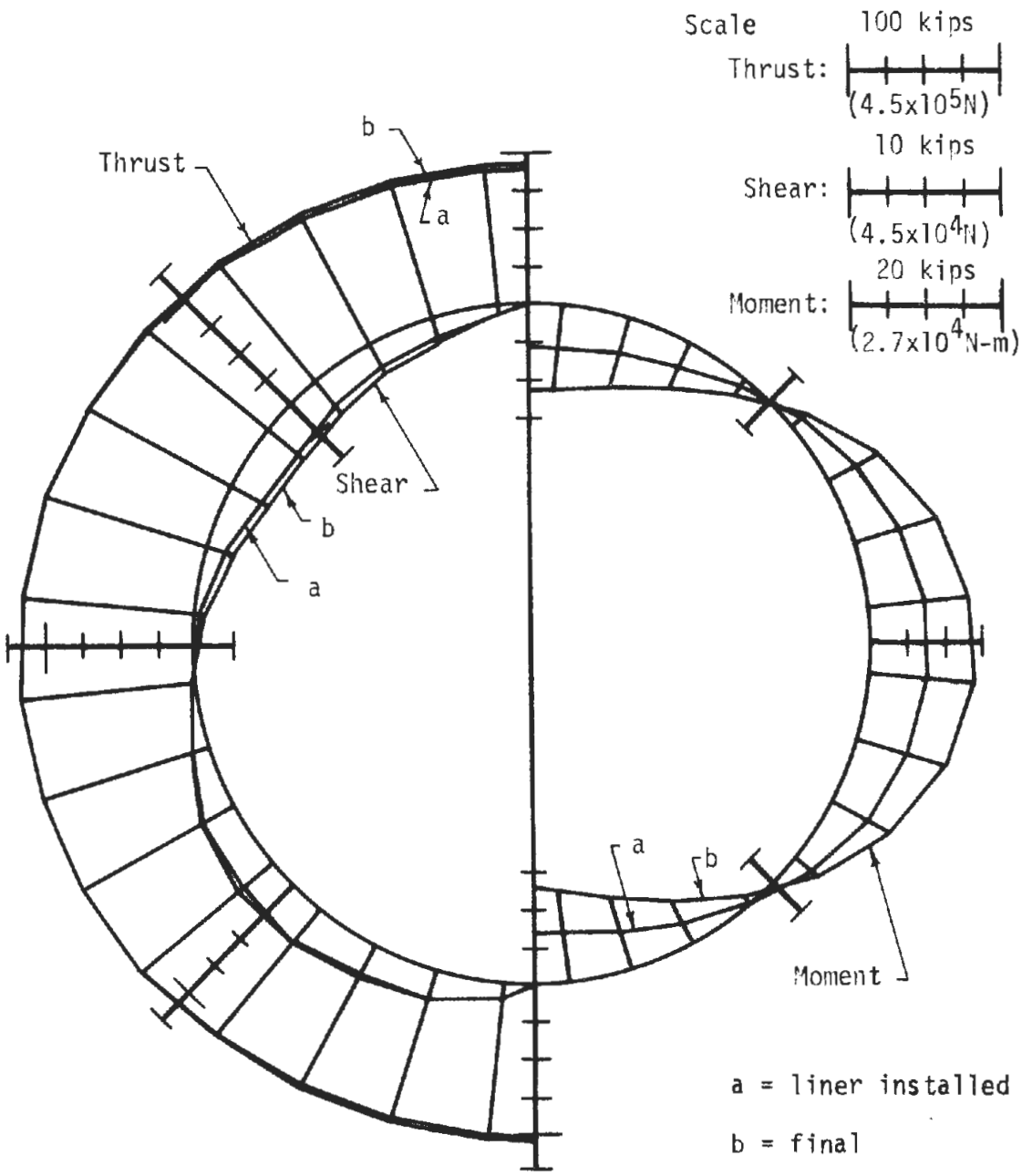

FIGURE 3.19 THRUST, SHEAR AND MOMENT DISTRIBUTIONS CALCULATED FOR TIME-DEPENDENT CASE 1

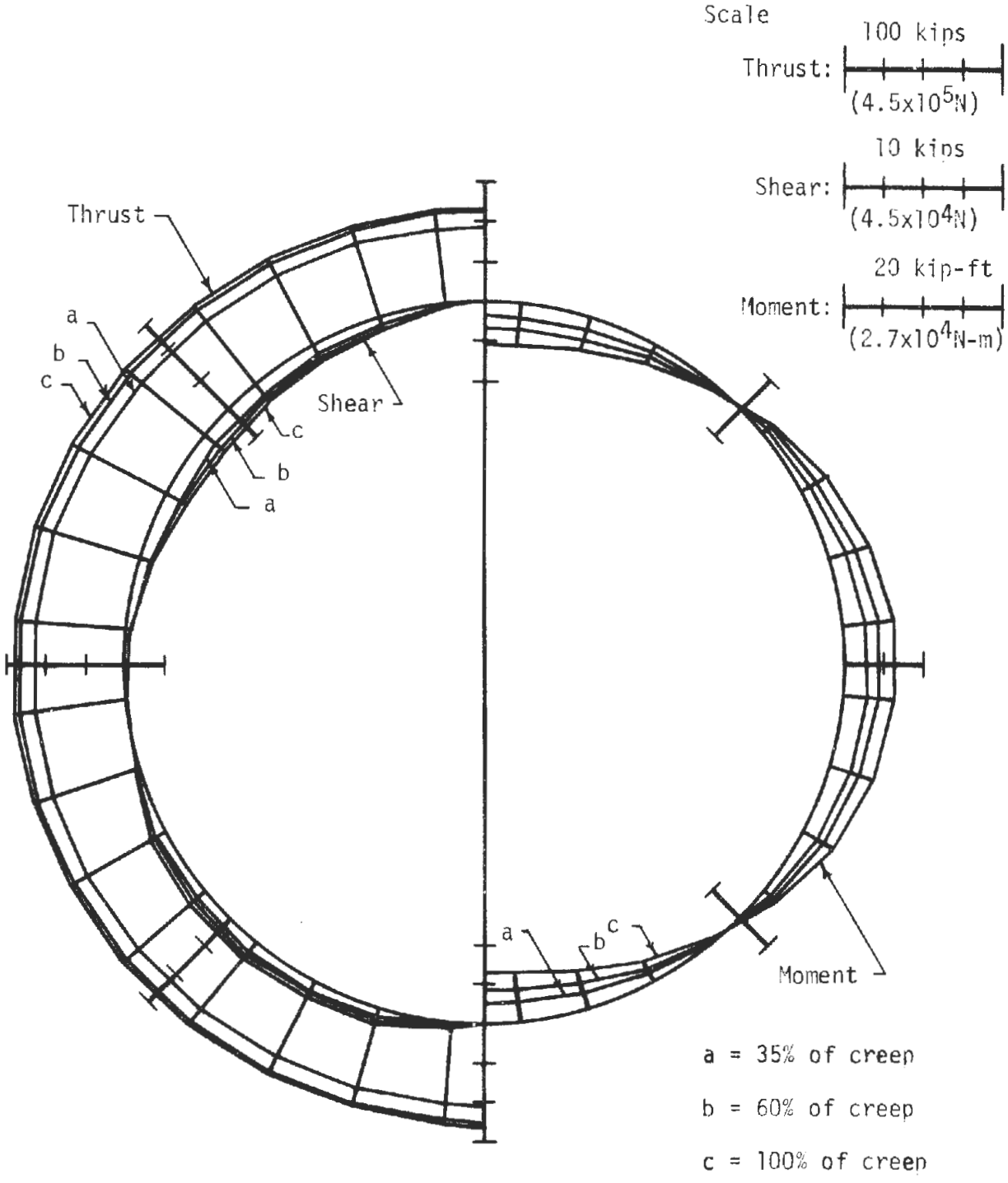

FIGURE 3.20 THRUST, SHEAR AND MOMENT DISTRIBUTIONS CALCULATED FOR TIME-DEPENDENT CASE 2

In Fig. 3.20 (case 2) the curves a, b and c are the thrust, bending and moment, and shear distributions for the times at which 35, 60 and approximately 100 percent of the total creep had occurred respectively. At time zero, prior to the initiation of creep, there were no liner forces because, as previously mentioned, there were no external stresses acting at that time. Thus, forces due to elastic behavior alone, such as in case 1, were here everywhere equal to zero. The force distributions in Fig. 3.20 are entirely the result of soil creep. As can be inferred from the creep curve (Fig. 3.7) changes in liner forces are initially large, but become smaller as time passes.

The above comparisons of these two time-dependent analyses with the linear-elastic case give some indication of the relative merits of performing a two-dimensional time-dependent analysis rather than a two-dimensional linear-elastic study when investigating tunnel support behavior. First, it appears that there is no need to consider time-dependent behavior if it is going to be assumed that the liner is installed simultaneously with instantaneous excavation. These assumptions tend to negate the possible time-dependent effects and give results very similar to those of the linear-elastic analysis. However, if it is to be assumed that the liner is to be installed only after a period of time has elapsed following excavation, the time dependent analysis is required because the linear-elastic analysis will indicate only that all liner forces are zero since the elastic deformations of the medium (instantaneous) occurred before the liner was placed.

CHAPTER 4

SUMMARY AND CONCLUSIONS

If an analytical model of an underground structure is to give realistic results it must take into consideration all stages of existence of the medium-structure system. In this study a method of analysis for underground structures using the finite element method has been outlined. The analysis has been divided into three phases, each representing a distinct stage under significantly different conditions.

In the initial phase of analysis the initial state of stress existing in the ground prior to excavation for the underground structure is determined. This is accomplished by the analysis of the pre-excavation configuration subject to the self weight of the medium and other possible types of loading such as tectonic stresses, residual stresses, or the weight of any existing surface structures. Next, in the construction phase of the analysis the actual sequence of excavation and construction to be considered is simulated. It is known that the method and details of excavation and construction can significantly influence the behavior of an underground structure and thus, it is of great importance that these factors be considered in any analysis. Finally, in the operation phase of the analysis the various loading conditions that are expected to arise during the useful life of the structure due to its operation or other factors can be considered.

Of major importance throughout the analysis are the material properties that control the behavior of the medium in which the structure is constructed. Five case studies which considered three different types of material behavior were conducted here utilizing the multi-stage analysis.

These analyses were intended to illustrate and provide an insight into the effect of material behavior properties on the performance of tunnel liners. The results obtained from the five cases considered are not sufficient to make any concrete conclusions that would be generally applicable to the wide range of possible cases. However, several inferences can be drawn that are applicable to the cases considered.

Examination of the external stress distributions for the linear-elastic and elasto-plastic cases shows that the final distribution of radical stresses acting on the liner was only slightly influenced by yielding of the medium. However, the shear stresses acting on the liner were significantly reduced when the medium was allowed to yield. Because of the relationship between external stresses and liner forces, these observations can be carried over to the consideration of liner thrust and moment. Differences between the liner-elastic case and the elasto-plastic cases indicated that thrust is fairly insensitive to small external stress changes due to yielding, whereas bending moments are sensitive to these changes, at least at certain points around the liner.

Those cases in which time dependent material behavior was considered were very interesting. When the liner was installed immediately upon excavation it was subjected to the full overburden pressure. The soil creep that followed had little effect on the thrust but significantly increased bending moments. The final force distributions that resulted, however, were very similar to those predicted by the linear-elastic analysis. This indicated that the time-dependent analysis has little to offer over the linear-elastic analysis, when considering long term response, if the time aspects of the construction sequence are not considered. When liner installation was delayed

a short time the final liner forces were appreciably reduced. This resulted because all the elastic deformations occurred before the liner was installed. Since, for most real tunnels, these deformations do occur before the liner can be placed, it seems that design procedures that do not account for this would be conservative.

If the stress and force distributions for all five cases are examined and compared the one thing that immediately becomes evident is that there really isn't much difference between them. This is unfortunate since it might lead to the conclusion that material behavior of the soil has little effect on liner performance. Actually, it is more likely that the similarity of results was due to some of the assumptions made in the analysis such as liner flexibility and time of installation. It seems reasonable to expect that the greater the extent of yielding or creep the greater will be the effect on the liner. The immediate installation of a fairly rigid liner acts to stabilize the system and reduce the extent of stress redistribution in the surrounding medium. Liner flexibility and time of liner placement are variables that must be examined more extensively. This means that future investigations must consider a wider range of material properties (liner flexibility) and, in some manner, account for the three-dimensional effects that influence the system ahead of the liner (time of liner placement).

Although the results obtained from this investigation remain tentative in terms of their use in design, they have provided an insight into the effects of material behavior on tunnel support performance and served as a guide to the most promising paths to follow in future investigations.

REFERENCES

1. *Analytical Modeling of Rock-Structure Interaction,* Vol. 1, Agbabian Assoc., Final Technical Report to U.S. Bureau of Mines, Contract H0220035, April 1973. (Order No. AD-761 648 from NTIS, Springfield, VA 22151)

2. Clough, R. W. and Woodward, R. J., III, "Analysis of Embankment Stresses and Deformations," *Journal of the Soil Mechanics and Foundation Division,* ASCE, Vol. 93, No. SM4, July 1967, pp. 529-549.

3. Christian, J. T. and Ing, H. W., "Errors in Simulating Excavation in Elastic Media by Finite Elements," *Soils and Foundations (Japan),* Vol. 13, No. 1, March 1973, pp. 1-10.

4. Desai, C. S., "Theory and Application of the Finite Element Method in Geotechnical Engineering," in *Symposium on the Application of the Finite Element Method in Civil Engineering,* U.S. Army Waterways Experiment Station, Vicksburg, Mississippi, 1972.

5. DiMaggio, F. L. and Sandler, I. S., "Material Models for Granular Soils," *Journal of the Engineering Mechanics Division,* ASCE, Vol. 97, No. EM3, June 1971, pp. 935-950.

6. Drucker, D. C. and Prager, W., "Soil Mechanics and Plastic Analysis or Limit Design," *Quarterly of Applied Mathematics,* Vol. 10, No. 2, 1952, pp. 157-165.

7. Drucker, D. C., Gibson, R. E. and Henkel, D. J., "Soil Mechanics and Work Hardening Theories of Plasticity," *Transactions,* ASCE, Vol. 122, 1957, pp. 338-346.

8. Duncan, J. M. and Dunlop, P., "Slopes in Stiff-Fissured Clays and Shales," *Contract Report No. TE 68-6,* U.S. Army Engineer Waterways Experiment Station, Vicksburg, Mississippi, June 1968.

9. Ghaboussi, J., Wilson, E. L. and Isenberg, J., "Finite Element for Rock Joints and Interfaces," *Journal of Soil Mechanics and Foundation Division,* ASCE, Vol. 99, No. SM10, October, 1973, pp. 835-848.

10. Kulhawy, F. H., Duncan, J. M. and Seed, H. B., "Finite Element Analysis of Stresses and Movements in Embankments During Construction," *Contract Report S-69-8,* U.S. Army Engineers Waterways Experiment Station, Vicksburg, Mississippi, November 1969.

11. Nelson, I., Baron, M. L. and Sandler, I., "Mathematical Models for Geologic Materials for Wave Propagation Studies," *DNA, Report No. 2672,* Washington, D. C.

12. Nelson, I. and Baron, M. L., "Development of Mathematical Models," *Report 5-68-1*, Contract DASA 38-67-C-0048, Paul Weidlinger Consulting Engineers, March 1968.

13. Paul, S. L., Gaylord, E. H., Hendron, A. J., Jr., Kesler, C. E., Mohraz, B. and Peck, R. B., *Research to Improve Tunnel Support Systems*, Report No. FRA-ORD&D 74-51, Federal Railroad Administration, Department of Transportation, June 1974. (Order No. PB-235-762/AS from NTIS, Springfield, VA 22151)

14. Peck, R. B., Hendron, A. J., Jr. and Mohraz, B., "State of the Art of Soft-Ground Tunneling," *Proceedings*, North American Rapid Excavation and Tunneling Conference, American Institute of Mining, Metallurgical, and Petroleum Engineers, New York, Vol. 1, Chapter 19, 1972, pp. 259-286.

15. Schofield, A. and Wroth, P., *Critical State Soil Mechanics*, McGraw-Hill, Ltd., 1968.

16. Wilson, E. L., Taylor, R. L., Doherty, W. P. and Ghaboussi, J., "Incompatible Displacement Models," in *ONR Symposium on Numerical Methods in Structural Mechanics*, Academic Press, 1971.

17. Zienkiewicz, O. C., Valliapan, S. and King, I. P., "Stress Analysis of Rock as a 'No-Tension' Material," *Geotechnique*, Vol. 18, 1968, pp. 56-66.

18. Zienkiewicz, O. C., *The Finite Element Method in Engineering Science*, McGraw-Hill, London, 1971.

19. Zienkiewicz, O. C. and Phillips, D. V., "An Automatic Mesh Calculation Scheme for Plane and Curved Surfaces by Isoparametric Coordinates," *Numerical Methods in Engineering*, Vol. 4, No. 3, 1971.

APPENDIX A

DESCRIPTION OF COMPUTER PROGRAM GEOSYS

A.1 GENERAL

The computer program GEOSYS is a general purpose computer program especially designed for the analysis of GEOtechnical SYStems.* This computer program uses the finite element method and has material nonlinearity options. The program is general purpose in the sense that its options allow analysis of a wide range of two and three dimensional getechnical problems with non-linear or time-dependent materials. The structure of the program is designed such that it provides the user a great degree of flexibility without sacrificing efficiency for the analysis of large problems.

A.2 THE STRUCTURE OF THE PROGRAM

The program GEOSYS is setup in three large sequential modules, each performing a main task in the analysis. The three modules are: Preprocessor, Solution and Postprocessor. The transfer of data between these modules takes place through peripheral storage units which are created at the end of each module. The three modules can be executed simultaneously or individually. Following are brief descriptions of the modules.

1. PREPROCESSOR--The input data defining the system to be analyzed is provided to preprocessor. The input data consists of: control data, data defining the geometry of the system, material data, loading and construction sequence data. All the

*This program was initially developed at Agbabian Associate, El Segundo, California, under a contract from U.S. Bureau of Mines, Spokane, Washington (1).

processing, generation, modification and display of data takes place in this module. In addition, some preliminary computations are carried out in the preprocessor which includes the determination of the shape functions and the derivatives of the shape function at the integration nodes.

2. SOLUTION--The solution module uses the data generated by the preprocessor and stored on a peripheral unit to solve the problem and compute the response of the system in a manner specified through control and loading data. Each cycle of the solution involves the following operations: computation of the strain increments, computation of the stresses and the tangent material property matrices, computation and assemblage of the internal resisting force vector, formation of the tangent stiffness matrix and the solution of the system of equations to determine the displacement increments. These operations fall into two categories; element level computations and global level computations. The global level computations involve the assemblage of the stiffness matrix and the load vector and the solution of the system of equations. The global level computations are carried out at three modes of operations selected by the program depending on the available core space. The smaller problems are core-resident; for the moderately large problems the stiffness matrix is formed in blocks, triangularized and transferred to peripheral storage; for the large problems the stiffness matrix is formed in blocks, transferred to peripheral storage units and after the completion of the stiffness formation, stiffness matrix

blocks are transferred back to core and triangularized. The response of the system is stored on a peripheral unit for the postprocessor.

3. POSTPROCESSOR--The function of the postprocessor is to process the response data, rearrange them and output in the appropriate form.

A.3 ELEMENT LIBRARY

The element library of the program contains a set of one, two and three dimensional elements which can be used in appropriate combinations to model any specific structure. The one dimensional bar and beam elements are, in general, in three dimensional space and have 6 and 12 degrees of freedom respectively. The two dimensional plane strain, plane stress and axisymmetric elements are 8 degree of freedom quadrilateral isoparametric (18) elements. The three dimensional element is an 8 node, 24 degree of freedom isoparametric element. The element library also includes a 16 node, 48 degree of freedom thickshell element (16). The two and three dimensional elements have additional degrees of freedom associated with the incompatible modes which are introduced in order to improve the bending properties of these elements (16). The additional incompatible degrees of freedom are eliminated at the element level.

The element library also includes a special joint element (9) for modeling of the behavior of the rock joints, faults and interfaces. The element is capable of simulating the slip and debonding along the joint surfaces.

A.4 MATERIAL LIBRARY

The material library is a module which is entered with the strain increments and the history of stresses and strains and in which the corresponding stresses and the tangent material property matrix are computed. This in itself is a nonlinear relation and therefore direct evaluation of the stresses and tangent material property matrix is not possible. For elasto-plastic materials first a check is made to determine if the current strain increment is purely elastic (initial elastic loading or unloading from a previously yielded state). In case the current strain increments are elasto-plastic, they are divided into smaller steps and the stresses are computed incrementally and the final stresses are used to compute the tangent material property matrix.

The material properties assigned to each element are identified by a material property number. Different material properties can be used simultaneously to model separate portions of a system. Different material models can also be combined. For example, the variable moduli model can be combined with elasto-plastic models. The resulting model will have variable moduli for the elastic portion of the strain increment and the yielding will take place according to the specified model.

The material library presently has the following material models.

1. Linearly elastic
2. Variable moduli
3. Elastic-perfectly plastic
4. Elastic-perfectly plastic with strain hardening cap

5. Visco-elastic

6. Visco-plastic

The rate independent models can be isotropic or anisotropic.

In addition to the above continuum models, a special material model is incorporated in the material library to simulate the material behavior of the joint (9): The capability exists for modeling of dilatant as well as nondilatant behavior of the joints.

A.5 SPECIAL OPTIONS

Simulation of Excavation and Construction--The process of excavation and construction is simulated in the program by switching elements off and on at appropriate steps. The element activity is provided by the input and each element is assigned two parameters specifying the steps in which the element is switched off to simulate excavation and the step in which the element is switched on, to simulate the construction.

Restart--Analysis of large nonlinear and time-dependent problems can involve numerous steps and a large amount of computer time. Such problems are usually executed at several stages to prevent any possible waste of computer time and also to provide more effective and flexible control of the solution. After each stage a restart tape is generated which contains all the information necessary for restarting and continuing the solution from where it was terminated at the previous step.

In the preprocessor restart options are provided in order to complete and check the input data before the execution. During the execution several

types of restart options are provided based on intervals of computer time or intervals of steps.

Rock Bolts--Rock bolts can be modeled by bar elements connecting the nodes which correspond to the ends of the rock bolt. Frictional rock bolts are modeled by connecting the bar element to the intermediate nodes as well. The element activity option can be used to switch on the bar elements at the appropriate step corresponding to installation of the rock-bolt. The prestressing of the rock bolts is modeled by inputing an initial stress in the bar element at the time of the installation.

A.6 USER-AID OPTIONS

Mesh Generator--The preparation of input data for the finite element mesh usually takes most of the engineering time which is spent in a finite element analysis. The mesh generator option of the program reduces this data preparation time considerably. This mesh generator, which was proposed by Zienkiewicz and Phillips (19), requires only a small amount of data to define a "key diagram" which consists of the main block of the mesh to be generated and the number of elements required per each block. With this minimum amount of data the program generates the nodal point coordinates, element connectivities, boundary conditions, tributary areas and load coefficients for the nodal points. After the generation of the mesh additional nodes, elements and boundary conditions, which cannot be generated, can be input manually.

With the appropriate definition of key diagram data it is possible

to generate meshes with curved boundaries and specified resolution of the elements. A detailed account of the mesh generator is given in Ref. 1.

Band-Width Reducer--The automatic generation of finite element meshes for certain cases results in a non-optimum band-width for the stiffness matrix which will require unnecessarily large computer time for the solution. In such cases the band-width reducer option of the program can be used to reduce the band width to an acceptable level. The band-width reducer does not minimize the band-width but often the computer time saved in the solution more than compensates the time spent in the band-width reduction.

Mesh Plot--The program has a plot package capable of producing plots of two and three dimensional meshes. A finite element mesh can be plotted from any viewing angle and any specified orientation along the paper. The viewing angle and the orientation is specified by inputing a "view vector" and a "horizon vector."

The mesh plot is very useful for visual checking of the mesh and also for interpretating results.